



**HAL**  
open science

## **A journey towards the forbidden zone: a new, cold, UHP unit in the Dora-Maira Massif (Western Alps)**

Paola Manzotti, Federica Schiavi, Francesco Nosenzo, Pavel Pitra, Michel Ballèvre

### ► To cite this version:

Paola Manzotti, Federica Schiavi, Francesco Nosenzo, Pavel Pitra, Michel Ballèvre. A journey towards the forbidden zone: a new, cold, UHP unit in the Dora-Maira Massif (Western Alps). *Contributions to Mineralogy and Petrology*, 2022, 177 (6), pp.59. 10.1007/s00410-022-01923-8 . insu-03695671

**HAL Id: insu-03695671**

**<https://insu.hal.science/insu-03695671>**

Submitted on 15 Jun 2022

**HAL** is a multi-disciplinary open access archive for the deposit and dissemination of scientific research documents, whether they are published or not. The documents may come from teaching and research institutions in France or abroad, or from public or private research centers.

L'archive ouverte pluridisciplinaire **HAL**, est destinée au dépôt et à la diffusion de documents scientifiques de niveau recherche, publiés ou non, émanant des établissements d'enseignement et de recherche français ou étrangers, des laboratoires publics ou privés.



Distributed under a Creative Commons Attribution 4.0 International License



# A journey towards the forbidden zone: a new, cold, *UHP* unit in the Dora-Maira Massif (Western Alps)

Paola Manzotti<sup>1</sup> · Federica Schiavi<sup>2</sup> · Francesco Nosenzo<sup>1</sup> · Pavel Pitra<sup>3,4</sup> · Michel Ballèvre<sup>3</sup>

Received: 11 February 2022 / Accepted: 16 May 2022  
© The Author(s) 2022

## Abstract

The distribution of ultrahigh-pressure metamorphism (*UHP*) at the scale of a mountain belt is of prime importance for deciphering its past subduction history. In the Western Alps, coesite has been recognized in the southern Dora-Maira Massif, in the lens-shaped Brossasco-Isasca Unit, but has not been found up to now in the other parts of the massif. We report the discovery of a new *UHP* unit in the northern Dora-Maira Massif (Western Alps), named Chasteiran Unit. It is only a few tens of metres thick and consists of graphite-rich, garnet–chloritoid micaschists, whose protoliths may be black shales of Silurian age. Garnet inclusions (chloritoid, rutile) and its growth zoning allow to precisely model the *P–T* evolution. Coesite crystals, which are pristine or partially transformed to palisade quartz occur as inclusions in the garnet outer cores. According to thermodynamic modelling, garnet displays a continuous record of growth during the prograde increase in *P* and *T* (25–27 kbar 470–500 °C) (stage 1), up to the coesite stability field (27–28 kbar 510–530 °C) (stage 2), as well as sub-isothermal decompression of about 10 kbar (down to 15 kbar 500–515 °C) (stage 3). The main regional, composite, foliation, marked by chloritoid and rutile, began to develop during this stage, and was then overprinted by chlorite–ilmenite (stage 4). The Chasteiran Unit is discontinuously exposed in the immediate hangingwall of the Pinerolo Unit, and it is located far away from, and without physical links to the classic *UHP* Brossasco-Isasca Unit. Moreover, it records a different, much colder, *P–T* evolution, showing that different slices were detached from the downgoing subduction slab. The Chasteiran Unit is the fourth and the coldest Alpine *UHP* unit known so far in the entire Alpine belt. Its *P–T* conditions are comparable to the ones of the Tian Shan coesite–chloritoid-bearing rocks.

**Keywords** Coesite · Ultra-high pressure · Continental subduction · Dora-Maira · Alps

## Introduction

Since the first discovery in the Italian Alps (Chopin 1984) and in the Norwegian Caledonides (Smith 1984), coesite is considered as the iconic mineral for ultrahigh-pressure (*UHP*) metamorphism. It is now known from many localities worldwide (Coleman and Wang 1995; Carswell and Compagnoni 2003; Chopin 2003; Gilotti 2013). Coesite-bearing metamorphic rocks represent deeply subducted oceanic and continental rocks, which occur in two main types of domains (Kylander-Clark et al. 2012). Large domains, typified by the Norwegian Caledonides (e.g., Wain 1997) and the Dabie Shan (e.g., Rolfo et al. 2004), display coesite-bearing rocks occurring over hundreds to thousands of square kilometres. Small domains, such as the Brossasco-Isasca Unit in the Dora-Maira Massif and the Cignana Unit in the Alps, show *UHP* rocks on a much smaller scale, of the order of a square kilometre (e.g., Compagnoni and Rolfo, 2003). This

---

Communicated by Hans Keppler.

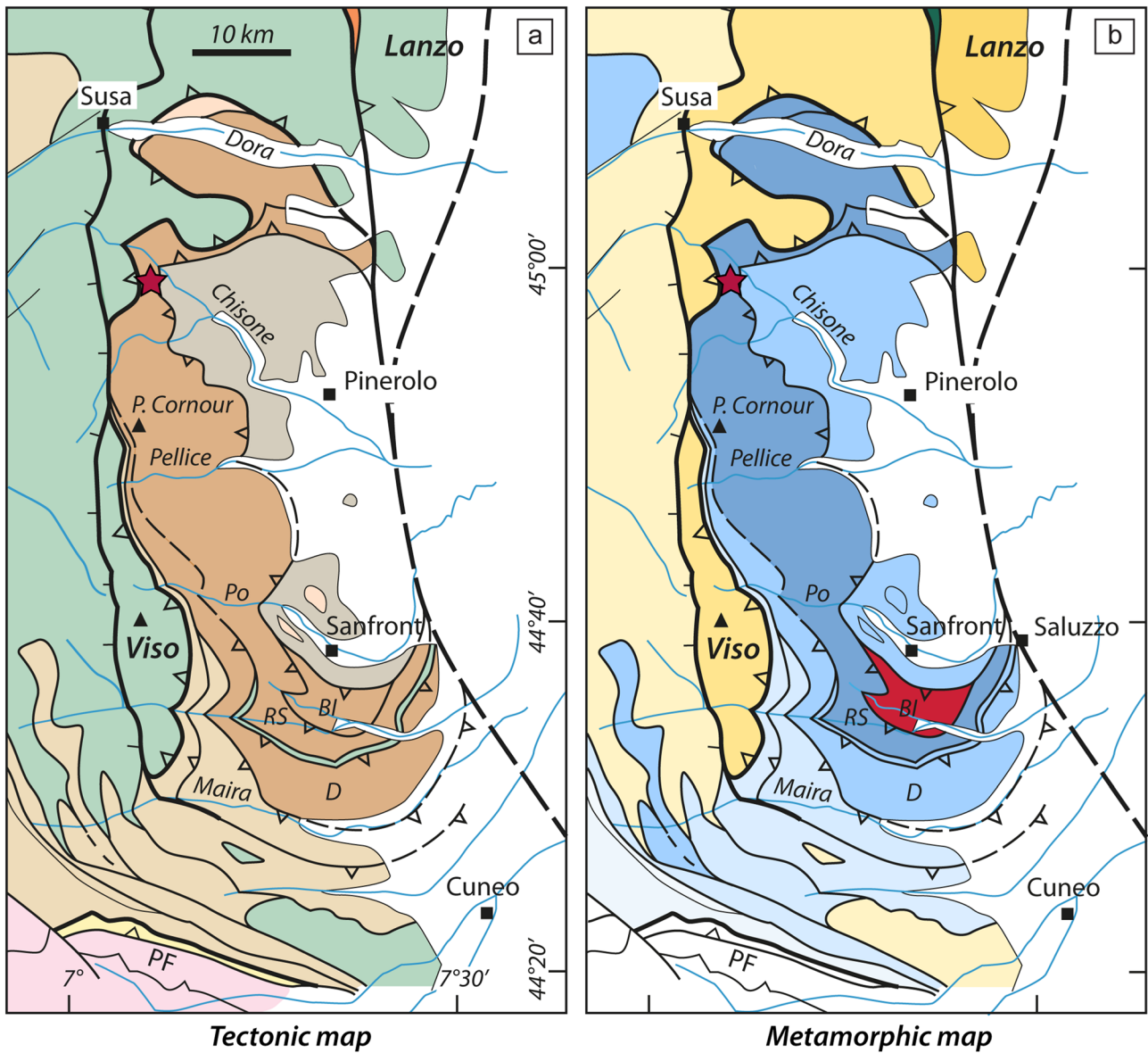
✉ Paola Manzotti  
paola.manzotti@geo.su.se

<sup>1</sup> Department of Geological Sciences, Stockholm University, 106 91 Stockholm, Sweden

<sup>2</sup> Université Clermont Auvergne, CNRS, IRD, OPGC, Laboratoire Magmas et Volcans, 63000 Clermont-Ferrand, France

<sup>3</sup> Univ Rennes, CNRS, Géosciences Rennes-UMR 6118, 35000 Rennes, France

<sup>4</sup> Česká geologická služba (Czech Geol. Survey), 118 21 Prague 1, Czech Republic



- Helvetic Domain**
- Subbriançonnais / Flysch**
- Briançonnais Domain**
- Dora-Maira Massif**
  - Mesozoic sediments
  - Carboniferous sediments & dioritic/granitic orthogneisses (Pinerolo - Sanfront)
  - Polycyclic basement + Permian intrusives (Brossasco-Isasca BI, Rocca Solei RS, Dronero D)
- Piemonte-Liguria Ocean**
- Adriatic Domain**

Late Cretaceous - Palaeocene  
80-60 Ma

Eclogite facies (Sesia Zone)

Early Eocene  
60-55 Ma

Blueschist facies (Queyras)

Eclogite facies (Lanzo)

Middle Eocene  
50-45 Ma

Eclogite facies (Viso)

Late Eocene  
40-35 Ma

law-ab facies

law-gl blueschist facies

g blueschist facies

q eclogite facies

coe-ky eclogite facies (BI)

**coe-ctd eclogite facies (Chasteiran)**

**Fig. 1** Simplified tectonic (a) and metamorphic (b) maps of the SW Alps (modified after Ballèvre et al. 2020). Colour coding refers to both metamorphic facies and ages. The red star indicates the location of the studied sample. *PF* penninic front

difference has implications for the potential exhumation mechanism of *UHP* rocks, and reveals that in some cases only a very small fraction of the subducted material went back to the surface. While exploring the structure and the history of the Dora-Maira Massif, focussing on its much less well-known northern part (Manzotti et al. 2016; Nosenzo et al. 2022), we discovered a new outcrop of coesite-bearing rocks that deserves a special attention for two main reasons. First, it is located far away from, and without physical links to the classic Brossasco-Isasca Unit. Second, the newly discovered *UHP* rocks indicate much lower *P–T* conditions (characterised by the association of coesite with almandine-rich garnet and Fe-rich chloritoid) than the Brossasco-Isasca rocks (where the stability field of chloritoid was largely exceeded during coesite stability). This paper is, therefore, devoted to a detailed description of these rocks, to properly characterize their *P–T* evolution and discuss the new constraint that they yield on the extent of the *UHP* units in the Western Alps.

## The Dora-Maira Massif in the Western Alps

The Dora-Maira, Gran Paradiso, and Monte Rosa Massifs in the Western Alps constitute the Internal Crystalline Massifs and belong to the distal part of the Briançonnais palaeomargin (Schmid et al. 2004; Handy et al. 2010; Ballèvre et al. 2020; Michard et al. 2022; Manzotti and Ballèvre 2022). They are made of slices of Palaeozoic basement and minor remnants of dismembered Mesozoic covers. The Dora-Maira Massif extends from the Susa valley in the north to the Maira valley in the south, over a length of ~70 km. The internal geometry of the southern Dora-Maira Massif is relatively well known (Fig. 1a): several tectonic units have been identified on the basis of lithological, structural and petrological data and they are separated by thrust sheets and slivers of Mesozoic meta-sediments and ophiolites (e.g., Chopin 1984; Chopin et al. 1991; Kienast et al. 1991; Compagnoni et al. 1995; Michard et al. 1995; Chopin and Schertl 1999; Compagnoni and Hirajima 2001; Rubatto and Hermann 2001; Compagnoni and Rolfo 2003 and refs therein; Compagnoni et al. 2012; Groppo et al. 2019; Bonnet et al. 2022; Michard et al. 2022). The Alpine metamorphism reached by these units varies from garnet blueschist (Dronero Unit), to quartz eclogite (Rocca Solei) to coesite eclogite facies (Brossasco-Isasca) conditions (Fig. 1b). For the lowermost unit of the nappe stack (i.e., Sanfront Unit), Alpine peak *P–T* conditions have been estimated at 14–16 kbar 400–500 °C

(Avigad et al. 2003) or 20–23 kbar 500–515 °C (Groppo et al. 2019).

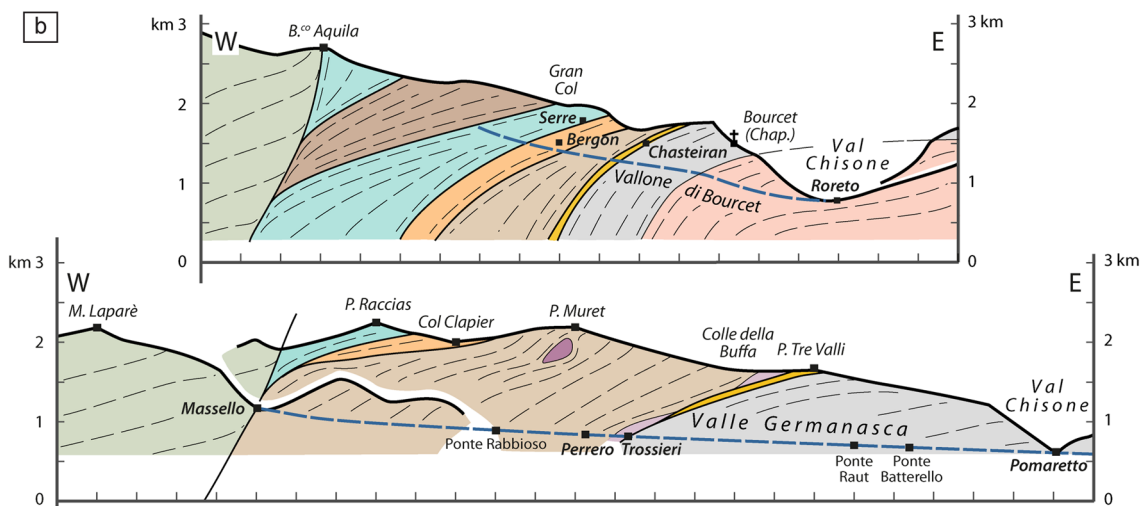
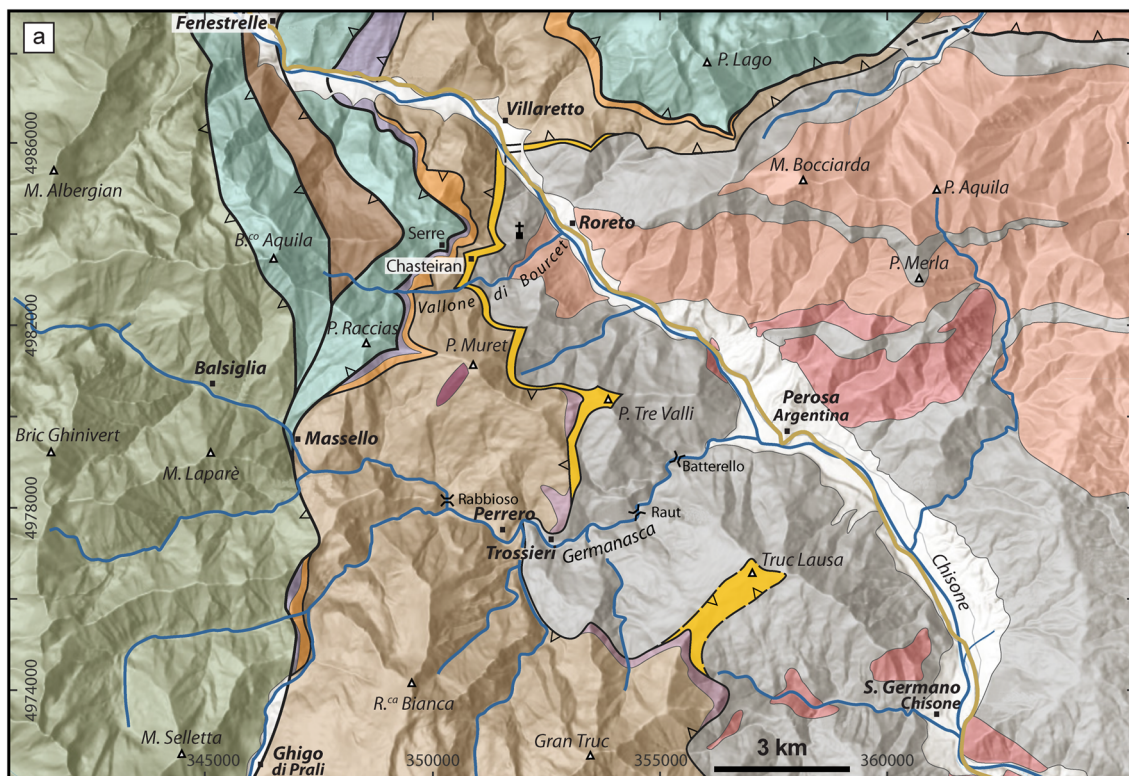
By contrast, very few studies have focused on the northern Dora-Maira Massif and little is known so far about its internal architecture and metamorphic evolution. There, the Pinerolo Unit is the structurally deepest unit of the Massif and comprises Upper Carboniferous graphite-rich meta-sediments intruded by Permian granites and diorites (Bussy and Cadoppi 1996; Manzotti et al. 2016). No *P–T* estimates have been done in this unit, although it is generally considered that it belongs to the upper blueschist facies (defined by chloritoid–phengite ± garnet assemblage in meta-sediments and glaucophane–epidote–garnet assemblage in mafic rocks, Bousquet et al. 2012).

In the northern Dora-Maira Massif, a single tectonic unit has been identified on top of the Pinerolo Unit (Borghi et al. 1996; Sandrone et al. 1993) and has been named the Muret Unit (Nosenzo et al. 2022). It mainly consists of polycyclic rocks (garnet micaschist intruded by an Ordovician granitoid, minor metabasite and marble) (Sandrone et al. 1993; Bussy and Cadoppi 1996; Cadoppi et al. 2016; Nosenzo et al. 2022). In this unit, Variscan Barrovian *P–T* conditions (6–7 kbar ~ 650 °C at 324 ± 6 Ma) have been recently characterised in a km-scale low strain domain (Nosenzo et al. 2022). A few bodies of Permian granitoids (e.g., Sangone monzogranite, Bussy and Cadoppi 1996) occur in the Muret unit. An Alpine mineral assemblage indicative of eclogite-facies conditions (garnet, omphacite, rutile) has been described (Borghi et al. 1985; Pognante and Sandrone 1989; Borghi and Sandrone 1990) and peak *P–T* conditions of 9–14 kbar ~ 500 °C have been estimated (Pognante and Sandrone 1989). According to Sandrone and Borghi (1992) and Borghi et al. (1996), the decompressional path of the Internal Crystalline Massifs was characterised by a first retrograde stage associated with moderate cooling at *P–T* conditions lower than the garnet stability field. This stage was followed by a re-heating (at 500–550 °C, on the basis of garnet–biotite geothermometer) at *P* < 5 kbar (on the basis of garnet–plagioclase–biotite–quartz geobarometer), resulting in the growth of a second generation of garnet, oligoclase rim around albite, calcic amphibole and replacement of chlorite by biotite in metapelites.

## Methods

### Textural observations, petrography, mineral and bulk-rock chemistry

Thin sections were studied with the optical microscope and backscattered electron (BSE) images. Chemical mapping of all garnet crystals including coesite (three porphyroblasts in two thin sections) as well as point analyses of all minerals



**Piemonte-Liguria Ocean**

- Dismembered ophiolites, minor meta-sediments (Orsiera-Raccias and Rocciavrè Units, eclogite-facies)
- Meta-sediments, minor ophiolites (Quyeras Unit, blueschist-facies)

**Dora-Maira Massif (?)**

**Fenestrelle Unit (HP)**

- Undifferentiated polycyclic basement and dismembered Mesozoic cover

**Dora-Maira Massif**

**Serre Unit (HP)**

- Dolomite, marble, calcschist, ankerite-micaschist (Mesozoic)
- Felsic gneiss (Permian?)

**Muret Unit (HP)**

- Polycyclic basement (micaschist, marble and garnet-blueschist)
- Granitic orthogneiss (undated)
- Granitic orthogneiss (Ordovician)

**Chasteiran Unit (UHP)**

- Graphite-rich, garnet-chloritoid micaschist

**Pinerolo Unit (HP)**

- Dioritic orthogneiss (Permian)
- Granitic orthogneiss (Permian)
- Graphitic meta-conglomerate and meta-sandstone (Upper Carboniferous)

present were performed using an electron microprobe. Details on the operating conditions are given in Table S1 (Supporting Information). Inclusions in garnet have been

carefully examined using Raman spectroscopy for phase identification in all thin sections (see paragraph ‘Raman spectroscopy of inclusions in garnet’ in the Supporting

**Fig. 2 a** Tectonic map of the northern Dora-Maira Massif in the Chisone and Germanasca valleys. The Chasteiran Unit (in yellow) is discontinuously exposed above the contact with the Pinerolo Unit. The geological map results from original fieldwork at 1:10,000 scale using the topographic base of the Carta Tecnica Regionale (CTR map) of the Piemonte region, Italy (coordinate system WGS84, UTM, zone 32 N) and by the integration of published geological maps (Mattiolo et al. 1913; Mattiolo et al. 1951 [reprinted]; Vialon 1966; Borghi et al. 1984; Cadoppi et al. 2002; Piana et al. 2017). Field data were digitized and projected on a digital topographic base (DTM of Piemonte region, <http://webgis.arpa.piemonte.it>). **b** W–E cross sections displaying the internal geometry of the northern Dora-Maira Massif and its structural relations with the overlying Piemonte–Liguria oceanic units. For sake of clarity, the Serre Unit is depicted with only one colour

Information for details on the method). Mineral abbreviations are those used by THERMOCALC (Holland and Powell 1998, Table S2, Supporting Information) along with a list of other symbols used in this study. Muscovite is used hereafter for all potassic white micas, whatever the Si content. Representative analyses of selected minerals are given in Tables S3, S4, and S5 (Supporting Information).

The bulk composition of sample CH11 (Table S6, Supporting Information) used for phase diagram calculations was determined by ICP–OES (CRPG, Nancy). A bulk-rock glass was prepared by mixing appropriate proportions (1:5) of fine-grained rock powder with di-lithium tetraborate. Details about the method used for the analyses are available in Carignan et al. (2001).

### Thermodynamic modelling

$P$ – $T$  pseudosections were calculated in the chemical system  $\text{MnO}–\text{Na}_2\text{O}–\text{CaO}–\text{K}_2\text{O}–\text{FeO}–\text{MgO}–\text{Al}_2\text{O}_3–\text{SiO}_2–\text{H}_2\text{O}–\text{TiO}_2–\text{Fe}_2\text{O}_3$  (MnNCKFMASHTO). Given the pelitic character of the studied sample, the amount of  $\text{Fe}^{3+}$  was set to 5% of total Fe [ $X(\text{Fe}^{3+}) = \text{Fe}^{3+}/\text{Fe}_{\text{total}}$ ], an arbitrary low value, considered appropriate for pelites (see Manzotti et al. 2018). The fluid phase was fixed as pure  $\text{H}_2\text{O}$ . Phase diagrams were calculated with the Theriak/Domino software (de Capitani and Brown 1987; de Capitani and Petrakakis 2010), using the internally consistent thermodynamic data set 6.2 (Holland and Powell 2011) and the suitable mixing models for solid solutions (converted for Theriak/Domino by D. K. Tinkham, <http://dtinkham.net/peq.html>). The phases considered in the calculations and the activity-composition models are given in Table S7 (Supporting Information).

Raman spectroscopy on carbonaceous material (RSCM, Beyssac et al. 2002) was applied to estimate the maximum  $T$  registered by the studied sample (details on the method are given in the paragraph ‘Raman spectroscopy on carbonaceous material (RSCM) method’ in the Supporting Information). Raman spectroscopy on quartz inclusions in garnet was performed to estimate the entrapment pressure of these

inclusions (using the calibration and the method described in Mazzucchelli et al. 2021). These two methods allow an estimation of  $T$  and  $P$ , respectively, which are independent from the equilibrium thermodynamics approach used by Theriak/Domino.

### The Chasteiran Unit in the northern Dora-Maira Massif

In the northern part of the Dora-Maira Massif, west of Torino (Fig. 2), the Chisone and Germanasca valleys carve deeply into the nappe stack. From top to bottom, the main tectonic units exposed in these valleys are:

- A blueschist-facies unit (Queyras Unit), part of the Piemonte–Liguria Ocean and essentially made of meta-sediments with subordinate dismembered ophiolitic bodies.
- Eclogite-facies units (Orsiera-Raccias and Rocciavré Units) derived from the Piemonte–Liguria Ocean and made of dismembered ophiolites (serpentinised peridotites, meta-gabbros and meta-basalts and minor meta-sediments).
- A polycyclic basement associated with a dismembered Mesozoic cover (Fenestrelle Unit) possibly part of the Dora-Maira Massif (Carraro et al. 2002).
- Felsic gneisses and associated volcano-sedimentary successions considered to be Permian in age, and remnants of a dismembered Mesozoic cover (mainly dolomites and marbles with minor calcschists and ankerite micaschists), discontinuously exposed at the contact with the oceanic units derived from the Piemonte–Liguria Ocean. These lithologies are hereafter referred to as the Serre Unit.
- A polycyclic basement unit belonging to the Dora-Maira Massif (Muret Unit). This unit consists of polycyclic micaschists, marbles and minor meta-basites, with an Ordovician orthogneiss. Relicts of pre-Alpine metamorphic assemblages (a first generation of garnet, staurolite, ilmenite) have been used to constrain its pre-Alpine history, culminating at 6 kbar, 650 °C, and dated at ~325 Ma (Nosenzo et al. 2022). In the micaschist, the Alpine metamorphism is recorded by the development of a second generation of garnet + chloritoid + Si-rich muscovite + rutile ± glaucophane.
- The Pinerolo Unit, the deepest structural unit of this part of the Dora-Maira Massif, is essentially made of Upper Carboniferous graphitic meta-conglomerates and meta-sandstones (Manzotti et al. 2016), intruded by Permian dioritic and granitic orthogneisses (Bussy and Cadoppi 1996).

Our detailed field mapping, aimed at characterising the contact between the Pinerolo Unit and the overlying Muret

Unit, has revealed the existence, at the contact between the two units, of a thin (10 to 50 m thick) layer of garnet–chloritoid micaschists (hereafter referred to as *Chasteiran Unit*, Fig. 2). The Chasteiran Unit is discontinuously exposed along the contact with the Pinerolo Unit, from the town of Villaretto in the Chisone Valley to the crest Truc Lausa in the Germanasca valley. The micaschist has a peculiar appearance, due to the numerous, strongly flattened, blackish lenses essentially consisting of chloritoid and metamorphosed carbonaceous material (hereafter called graphite), alternating with whitish, quartz- and mica-rich lenses. Garnet is dispersed in the rock as idioblastic or sub-idioblastic grains 1 to 5 mm in diameter. The main composite foliation, which wraps around garnet porphyroblasts, is parallel to the contact between the Pinerolo and Muret Units. We collected a large number of samples from all units (a total of 250 samples). One sample (CH11) collected close to the Chasteiran church attracted our attention, because, in thin section, there were radiating cracks around quartz polycrystalline inclusions in garnet, a potential indication of the former presence of coesite (e.g., Chopin, 1984; Boyer

et al., 1985). Consequently, we have done many thin sections in this sample (Tab. S8 in the Supporting Information) and indeed we were able to positively identify coesite in two of them. Therefore, the present study aims to characterize the petrological evolution of the Chasteiran Unit, whereas following papers will detail its field relations, geometry, and geochronology (work in progress).

### Petrography and mineral chemistry

Sample CH11 (from the type locality of the unit, namely, Chasteiran, Lat/Long coordinates 44° 59' 21.75" N–7° 06' 29.03" E; Figs. S1, S2) is dark grey in colour and consists of muscovite (20–30%), quartz (15–20%), chloritoid (15–20%), garnet (5–10%), chlorite (5–10%), paragonite (5–10%), graphite (5–10%), as well as minor rutile, ilmenite, epidote, albite and, importantly, coesite. Accessory tourmaline also occurs (Fig. 3).

The main composite foliation is defined by the alternation of mm-thick layers of either muscovite + graphite or chloritoid + graphite, which are parallel to elongated quartz

	STAGE 1	STAGE 2	STAGE 3	STAGE 4
Mineral	<i>g inner core</i>	<i>g outer core</i>	<i>g rim / foliation</i>	<i>pseudomorphs, overgrowths on foliation</i>
q				
coe				
mu	Si 3.49–3.50 a.p.f.u.	Si 3.40–3.45 a.p.f.u.	Si 3.30–3.37 a.p.f.u.	
g	alm <sub>75-78</sub> spss <sub>12-9</sub> py <sub>6-7</sub> grs <sub>5-6</sub>	alm <sub>79-80</sub> spss <sub>8-3</sub> py <sub>7-9</sub> grs <sub>5-9</sub>	alm <sub>80-67</sub> spss <sub>3-1</sub> py <sub>9-3</sub> grs <sub>9</sub> →30 →22	
ctd	X <sub>Mg</sub> 0.14–0.15	X <sub>Mg</sub> 0.16–0.18	X <sub>Mg</sub> 0.16–0.18	X <sub>Mg</sub> 0.09–0.12
chl				X <sub>Mg</sub> 0.31–0.34
law			— — — —	
ep			— — — — —	
jd	?	?		
gl	?			
pa			— — — —	
ab				
ru				
ilm				
tur				
gph				

**Fig. 3** Deformation/mineral growth relationships for sample CH11. Grey lines indicate pseudomorphed minerals. Question marks refer to phases that may have been present according to the phase diagram modelling, but for which no petrographic evidence has been found

lenses (Figs. S2, S3, S4). Within the layers, muscovite, chloritoid, rutile, and ilmenite/rutile display a strong shape preferred orientation. Muscovite marking the main foliation shows chemical zoning (Fig. S5), with decreasing Si content and  $X_{Mg}$  and increasing  $X_{Na}$  from core (Si = 3.40–3.45 a.p.f.u., locally up to 3.50 a.p.f.u.;  $X_{Na}$  = 0.01–0.04; and  $X_{Mg}$  = 0.67–0.72) to rim (Si = 3.30–3.37 a.p.f.u.;  $X_{Na}$  = 0.04–0.05; and  $X_{Mg}$  = 0.52–0.60). Chloritoid aligned along the main foliation is zoned (Fig. S6) with a magnesium-rich core ( $X_{Mg}$  = 0.16–0.18) and more iron-rich rim ( $X_{Mg}$  = 0.09–0.12). Chloritoid cores contain inclusions of rutile, whereas chloritoid rims are in contact with ilmenite.

Idioblastic porphyroblasts (up to 5 mm in size) of garnet are found in high-Si muscovite layers (Fig. 4) and they are wrapped by the matrix foliation. Garnet crystals are optically zoned and display large (up to 4.5 mm-thick) colourless cores and thin (up to 500  $\mu$ m-thick) light pink rims. Inclusions are mainly concentrated in garnet inner cores, whereas they are less abundant in garnet outer cores and rims (Figs. 4, 5a). Garnet inner cores contain monocrystalline inclusions of chloritoid ( $X_{Mg}$  = 0.14–0.15, Figs. S6 and S7a), rutile, quartz, and tourmaline, and polymineralic aggregates of paragonite ( $X_{Na}$  = 0.90–0.98) + minor epidote ( $Fe^{3+}/[Al^{3+} + Fe^{3+}] = 0.07–0.08$ )  $\pm$  muscovite (Si = 3.28–3.37

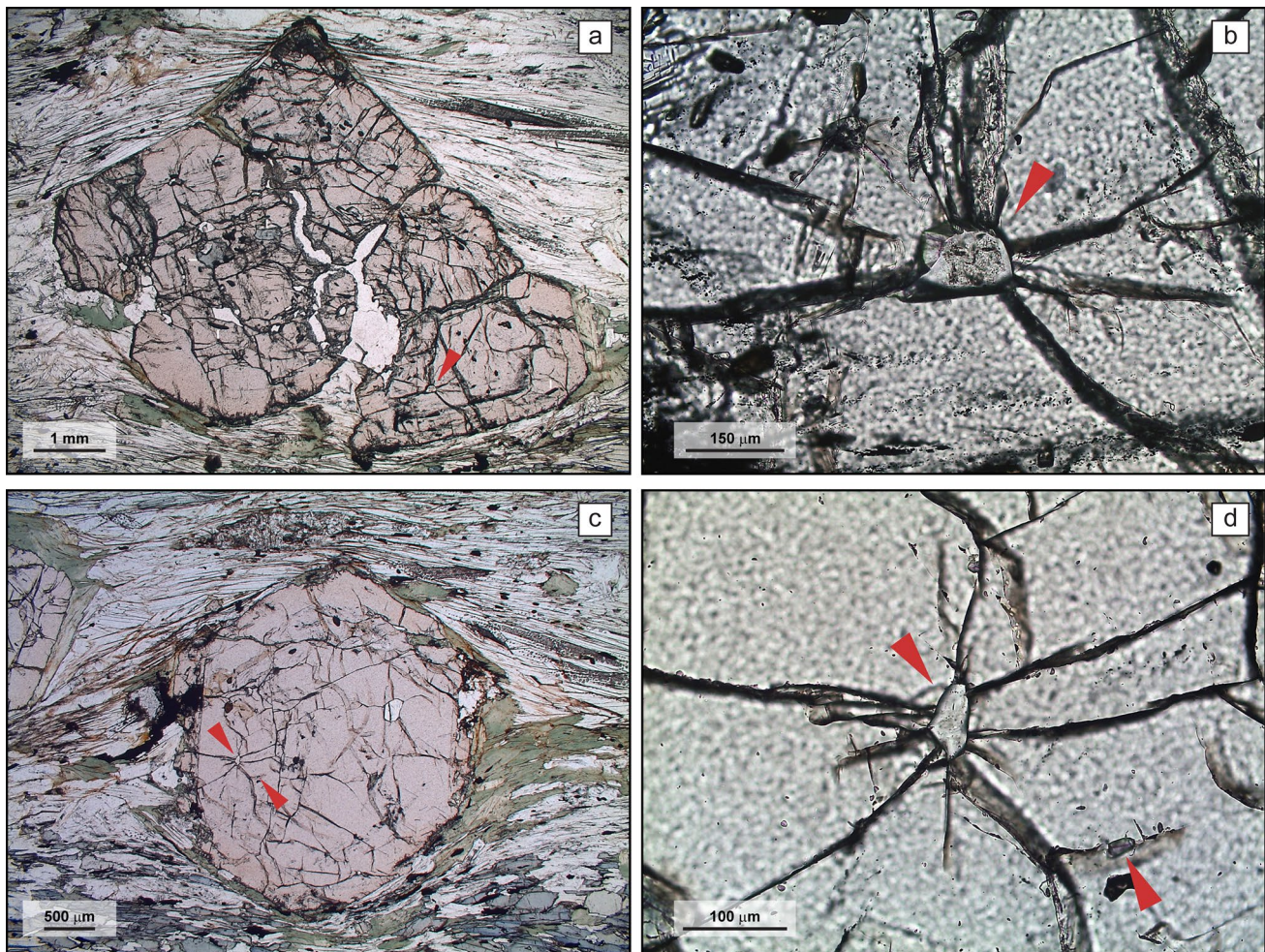


**Fig. 4** Photomicrographs (plane-polarised light) for sample CH11. **a** Fractured garnet porphyroblast wrapped by the matrix foliation. Numerous inclusions of chloritoid, quartz, and rutile occur in the inner core, whereas garnet outer core displays only a few inclusions of coesite (red arrow) and rutile. Inclusions are almost absent in garnet rim, with the exception of a few rutile crystals. **b** Close-up of the coesite inclusion (partially transformed to quartz) enclosed in garnet, shown in (a). Note the radial fractures around the inclusion in the host garnet and the higher relief of coesite with respect to quartz. **c** Garnet porphyroblast with a coesite inclusion in the outer core (red

arrow right) and a polycrystalline aggregate of quartz surrounded by radial cracks (red arrow left). Garnet is partially replaced by chlorite at the rim. The matrix foliation is marked by chloritoid and high-Si muscovite and wraps around garnet. **d** Enlargement of the coesite included in garnet outer core. A tiny ( $\sim 10$   $\mu$ m in size) coesite inclusions is surrounded by a narrow quartz rim (see also Fig. S2 in the Supporting Information). Radial cracks developed in the host garnet around a coesite inclusion ( $\sim 30$   $\mu$ m in size) that is completely transformed to quartz

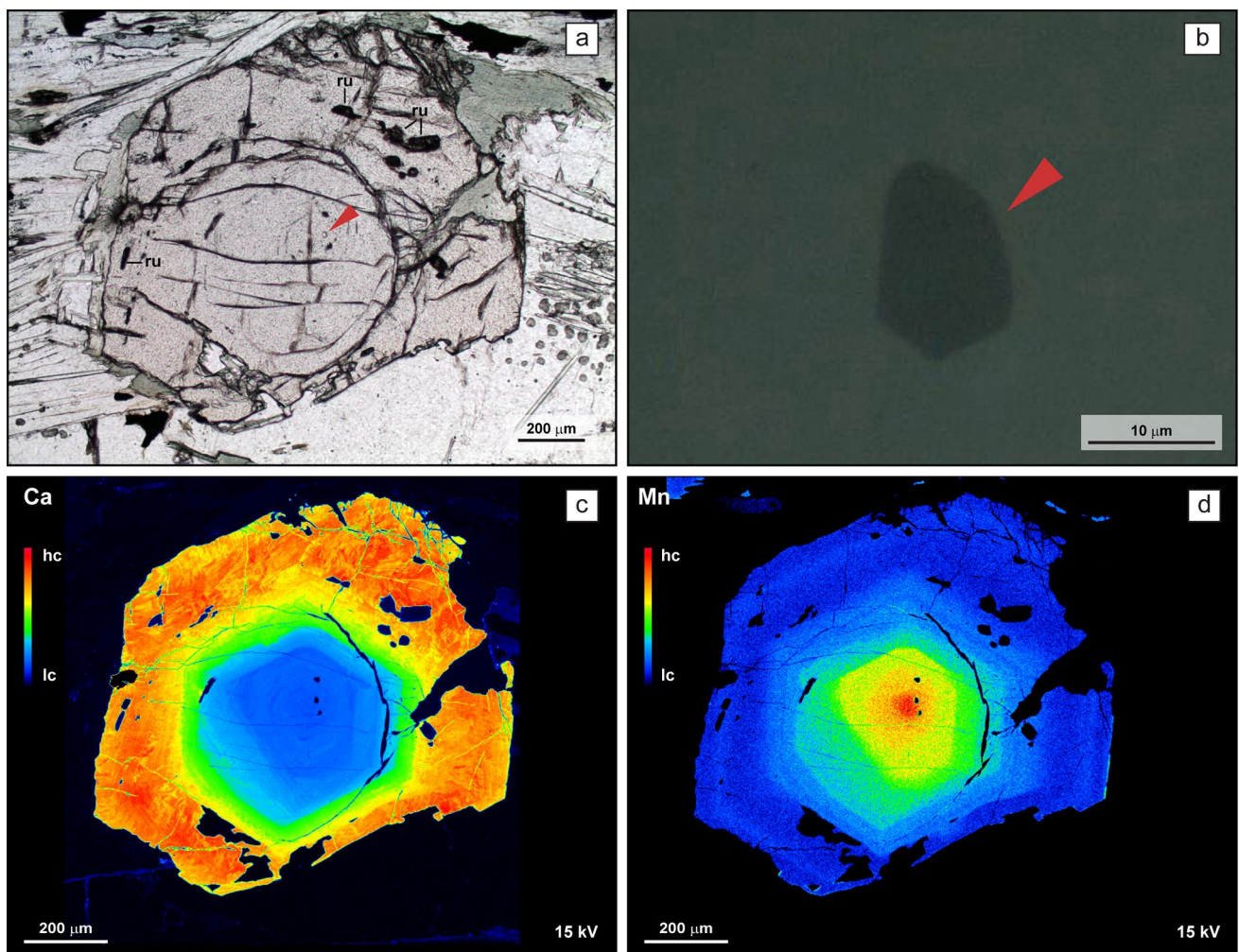


**Fig. 5** **a** Photomicrograph (plane-polarised light) of a garnet porphyroblast displaying rutile inclusions in the core and rim. The red arrow indicates a coesite inclusion. **b** Enlargement (reflected light) of

the tiny ( $\sim 10 \mu\text{m}$  in size) pristine coesite inclusion in garnet with no radial cracks **c**, **d** X-ray maps of Ca and Mn

a.p.f.u.;  $X_{\text{Na}}=0.04\text{--}0.06$ ; and  $X_{\text{Mg}}=0.47\text{--}0.55$ ; Figs. S5 and S7b). These aggregates may be interpreted as pseudomorphs after lawsonite, as reported in other high-pressure metapelite from the Dora-Maira Massif (e.g., Groppo et al. 2019). Garnet outer cores contain inclusions of coesite (Figs. 6, S8 see below), polycrystalline aggregates of quartz, and rare monomineralic inclusions of chloritoid ( $X_{\text{Mg}}=0.16\text{--}0.18$ , Fig. S6) graphite, and rutile (Figs. 4, 5). A few polyminerallitic inclusions consisting of paragonite ( $X_{\text{Na}}=0.90\text{--}0.98$ ) + minor epidote ( $\text{Fe}^{3+}/[\text{Al}^{3+} + \text{Fe}^{3+}]=0.12\text{--}0.15$ ) are also observed in this domain. Rare monomineralic inclusions of rutile, quartz, tourmaline, and epidote occur in garnet rims (Figs. 5a, S7c).

Garnet cores display growth zoning (Figs. 5c, d, 7, 8, 9), with a decrease in spessartine (from 12 to 3 mol%) compensated by an increase in almandine (from 75 to 80 mol%), pyrope (from 6 to 9 mol%) and grossular (from 5 to 9 mol%). Despite the similarity of the absolute values, however,

pyrope and grossular zoning display subtle, but significant differences. The grossular content remains approximately constant over the inner core and most of the outer core ( $\sim 5\text{--}6$  mol%) and increases significantly at the outermost core. On the other hand, the increase of the proportion of pyrope is continuous from the centre of the core to the edge of the outer core.

Garnet rim shows an abrupt decrease in almandine (from 80 to 67 mol%) and spessartine (from 3 to 1 mol%). Grossular strongly increases (from 9 to 29–30 mol%) and then slightly decreases (from 29–30 to 22 mol%). Pyrope mostly decreases (from 9 to 3 mol%). However, locally a slight increase is observed in the outermost rim (Fig. 9, right rim of profile G–H). X-ray mapping shows that in this domain Ca locally displays patchy zoning (Fig. 5c).

The garnet chemical composition close to the coesite inclusions (measured in the three

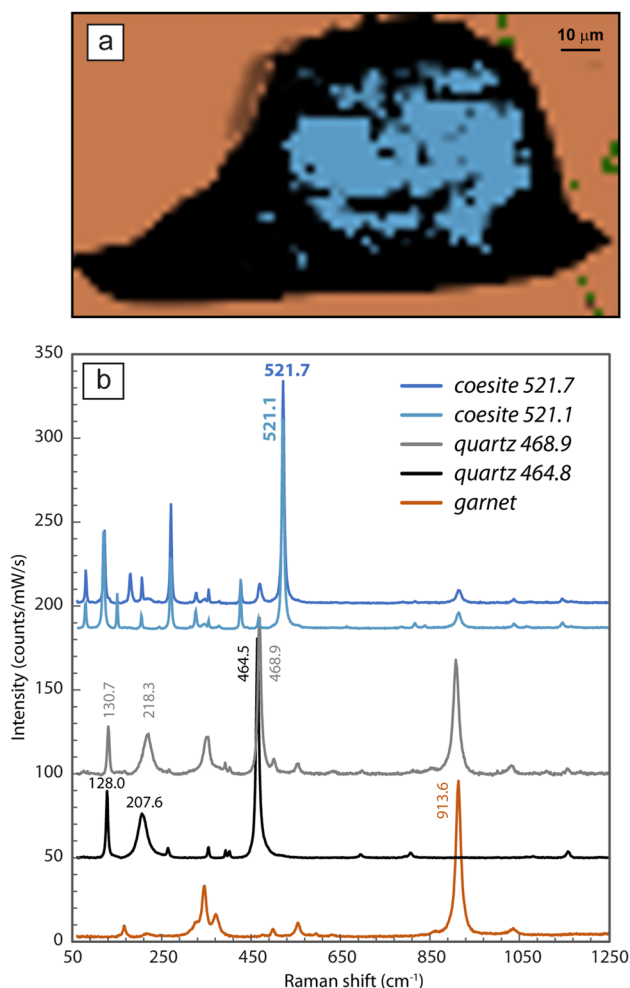


**Fig. 6** **a** Raman map showing the distribution of coesite (light blue), quartz (in black), garnet (in orange), and chlorite (in green). Coesite is included in the garnet porphyroblast shown in Fig. 4a, **b** From top to bottom: Raman spectra of coesite (main peak at  $\sim 521$   $\text{cm}^{-1}$ ) and quartz (main peak at  $464$ – $469$   $\text{cm}^{-1}$ ) hosted in garnet (main peak at  $\sim 915$   $\text{cm}^{-1}$ ) outer core. Spectra are offset for clarity

garnet porphyroblasts, where coesite has been identified) is  $\text{alm}_{80-81}\text{-prp}_7\text{-grs}_6\text{-spss}_6$  (Tab. S3 in the Supporting Information) and corresponds to the composition of garnet outer core. It is likely, therefore, that the garnet section shown in Fig. 5 does not pass through the centre (i.e., the inner core) of the crystal. Alternatively, garnet crystals may have nucleated at different stages during the history of the rock.

No optical discontinuity (beyond the colour change) separates garnet outer cores from garnet rims. X-ray mapping shows that the interface between garnet outer cores and rims is regularly shaped with only very rare and small embayments (Figs. 5c, d, 7 and 8). One garnet crystal displays mm-long fractures (up to 200  $\mu\text{m}$ -thick) filled by quartz (Figs. 4a, 7) and dissecting the garnet crystal in several fragments (from 1 to 2 mm in size). X-ray mapping reveals that the walls of the fractures are overgrown by a thin layer of a

new garnet with the composition of garnet rim (Fig. 7). Most garnet crystals display narrow fractures filled by chlorite.

Lozenge-shaped pseudomorphs occur in quartz-rich domains and consist of chlorite + albite + quartz (Fig. S7d). Their shape and replacement minerals suggest that they represent pseudomorphs after sodic amphibole, as reported in other high-pressure Alpine units (e.g., Compagnoni, 1977; Manzotti et al. 2021; Nosenzo et al. 2022). Rare albite porphyroblasts overgrow the foliation. Rutile in the matrix is partially rimmed by ilmenite. Garnet is partially replaced by chlorite ( $X_{\text{Mg}} = 0.31$ – $0.34$   $X_{\text{Mn}} = 0.001$ – $0.003$ ) both at the rims and along fractures. Paragonite ( $X_{\text{Na}} = 0.93$ – $0.95$ ) and chlorite ( $X_{\text{Mg}} = 0.32$ – $0.33$   $X_{\text{Mn}} = 0.002$ ) statically overgrow the main foliation.

To sum up, the following mineral assemblages developed during garnet growth (Fig. 3):

garnet inner cores + quartz + muscovite + chloritoid + lawsonite + rutile (stage 1); garnet outer cores + coesite + muscovite + chloritoid + lawsonite + rutile (stage 2); garnet rims + quartz + muscovite + chloritoid  $\pm$  epidote + glaucophane + rutile (stage 3). Lawsonite and glaucophane were completely replaced by retrograde phases that developed during stage 3 or 4.

### Coesite inclusions in garnet

Coesite occurs either as tiny pristine crystals ( $\sim 10$   $\mu\text{m}$  in size) without radial cracks in the garnet host (Fig. 5), or as larger crystals (up to  $\sim 100$   $\mu\text{m}$  in size) partially transformed to palisade quartz (Figs. 4, 6a, S8). Coesite partially transformed to quartz is surrounded by radial cracks that result from the volume increase related to the coesite–quartz transformation (Fig. 4b,d). Micro-Raman investigations on exposed inclusions (Fig. 6) confirm the presence of coesite, which displays the diagnostic Raman spectrum, characterized by more than fifteen vibrational modes (e.g., Hemley 1987; Gillet et al. 1990) with the most intense band at  $521$   $\text{cm}^{-1}$  (Fig. 6b). Mixed Raman spectra of coesite and quartz were measured in coesite crystals partially transformed to quartz. A tiny coesite inclusion surrounded by a thin ( $< 3$   $\mu\text{m}$ ) quartz shell (Figs. 4d and S8a) displays a slight Raman shift of its main coesite band ( $\nu = 521.7$   $\text{cm}^{-1}$ , Fig. 6b) indicating that a residual pressure is retained by the coesite inclusion in the garnet. A residual pressure is also recorded by the shift in the main Raman band of quartz measured in this shell around coesite ( $\nu = 466.8$   $\text{cm}^{-1}$ ; Fig. 6b, Table S12 and Fig. S8 in the Supporting Information). Raman mapping confirms the presence of quartz replacing coesite at the inclusion–host interface, as well as minuscule relict coesite within quartz (Fig. 6a). Quartz observed within coesite may be associated with thin veinlets, as observed in coesite inclusions in garnet from other UHP terranes (e.g., Korsakov et al. 2007).

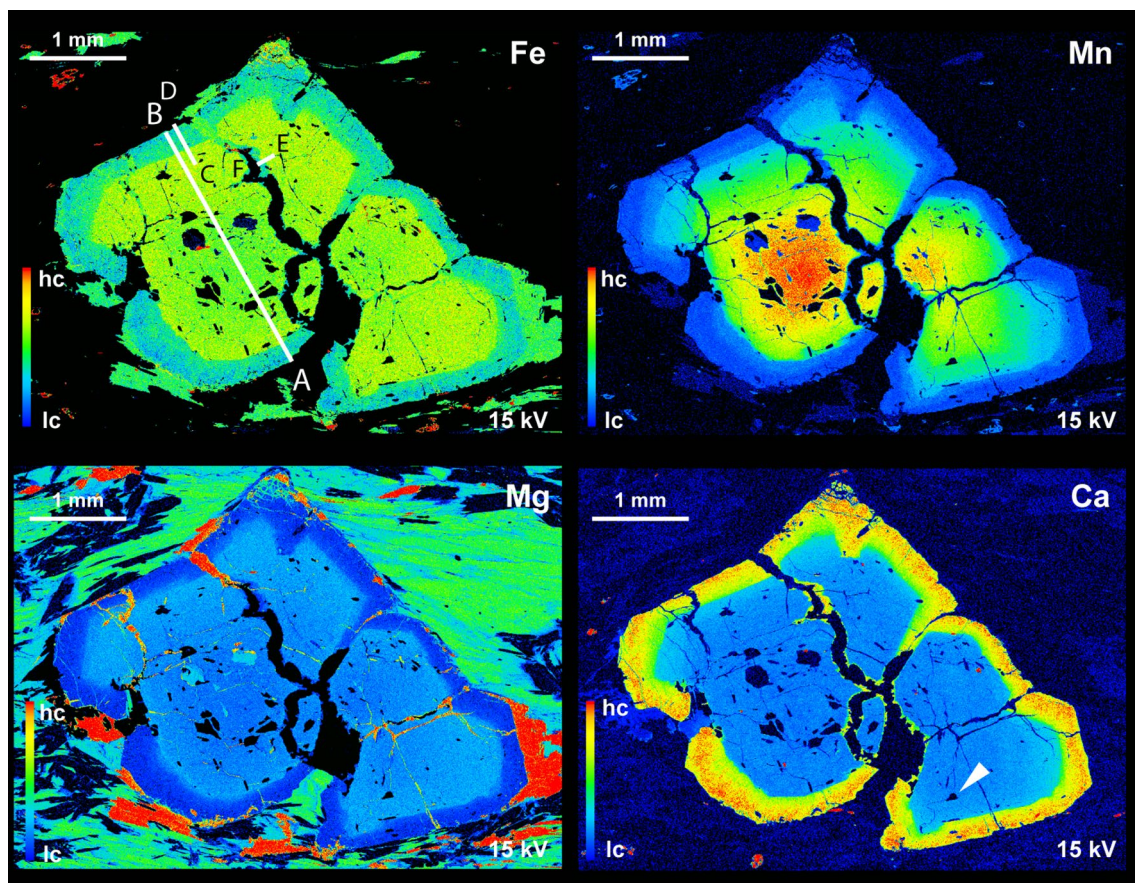


**Fig. 7** X-ray maps of a garnet from sample CH11. Fractures dissect garnet core and are sealed by quartz and by a garnet that has the same composition as the garnet rim. Therefore, fractures are interpreted to have developed before the growth of garnet rim. The interface between garnet core and garnet rim is regular, suggesting no or lim-

ited dissolution of garnet core before the growth of garnet rim. The white arrow in the Ca map indicates a coesite relict surrounded by a thin rim consisting of a polycrystalline quartz aggregate (see also Figs. 4 and 6)

### Elastic barometry using quartz inclusions in garnet

We collected 64 Raman spectra on exposed quartz grains included in the cores and rims of 15 garnet crystals (Fig. S8, Tab. S12 in the Supporting Information). Negligible or low residual pressures are retained in a large number of quartz inclusions. The largest residual pressure (highest Raman shift for quartz band is  $468.8 \text{ cm}^{-1}$ ) is provided by a sub-rounded, fracture-free quartz inclusion ( $< 5 \mu\text{m}$  in size) located in the garnet rim. The entrapment conditions have been calculated from the residual strain measured in this inclusion, following Mazzucchelli et al. (2021). The residual pressure ( $P_{\text{inc}}$ ) obtained using the EoS of the inclusion is  $P_{\text{inc}}^{\text{V}} = 5.44 \pm 0.16 \text{ kbar}$ , whereas the residual pressure calculated using the strain through the stiffness tensor is  $P_{\text{inc}}^{\text{strain}} = 5.09 \pm 0.09 \text{ kbar}$ . The isomeke calculated from the  $P_{\text{inc}}^{\text{V}}$  and  $P_{\text{inc}}^{\text{strain}}$  provides a pressure of  $P_{\text{trap}} = 14.3 \pm 0.2 \text{ kbar}$  at  $520 \text{ }^\circ\text{C}$  and of  $P_{\text{trap}} = 13.7 \pm 0.2 \text{ kbar}$  at  $520 \text{ }^\circ\text{C}$ , respectively (Table S13). Because the analysed inclusion was exposed,

it is likely that a relaxation of residual pressure may have taken place. Therefore, this  $P$  estimate should be considered as minimum value. Similar residual pressures of max 5 kbar were measured in unexposed coesite grains in the Lago di Cignana Unit in the Western Alps (Taguchi et al. 2021).

### RSCM temperature

RSCM temperatures were estimated on two thin sections (CH11 and CH11-5) cut from sample CH11 (results are given in Table S9 and Fig. S9 in the Supporting Information). Similar  $T$  (CH11 =  $486 \pm 19 \text{ }^\circ\text{C}$ , CH11-5 =  $481 \pm 15 \text{ }^\circ\text{C}$ ) are estimated in the two thin sections, with an average of  $483 \pm 17 \text{ }^\circ\text{C}$ . Graphite yields rather constant  $R^2$  values in the range 0.25–0.40 with the exception of two crystals characterised by higher  $R^2$  values ( $R^2 = 0.44$  in CH11 and  $R^2 = 0.45$  in CH11-5).

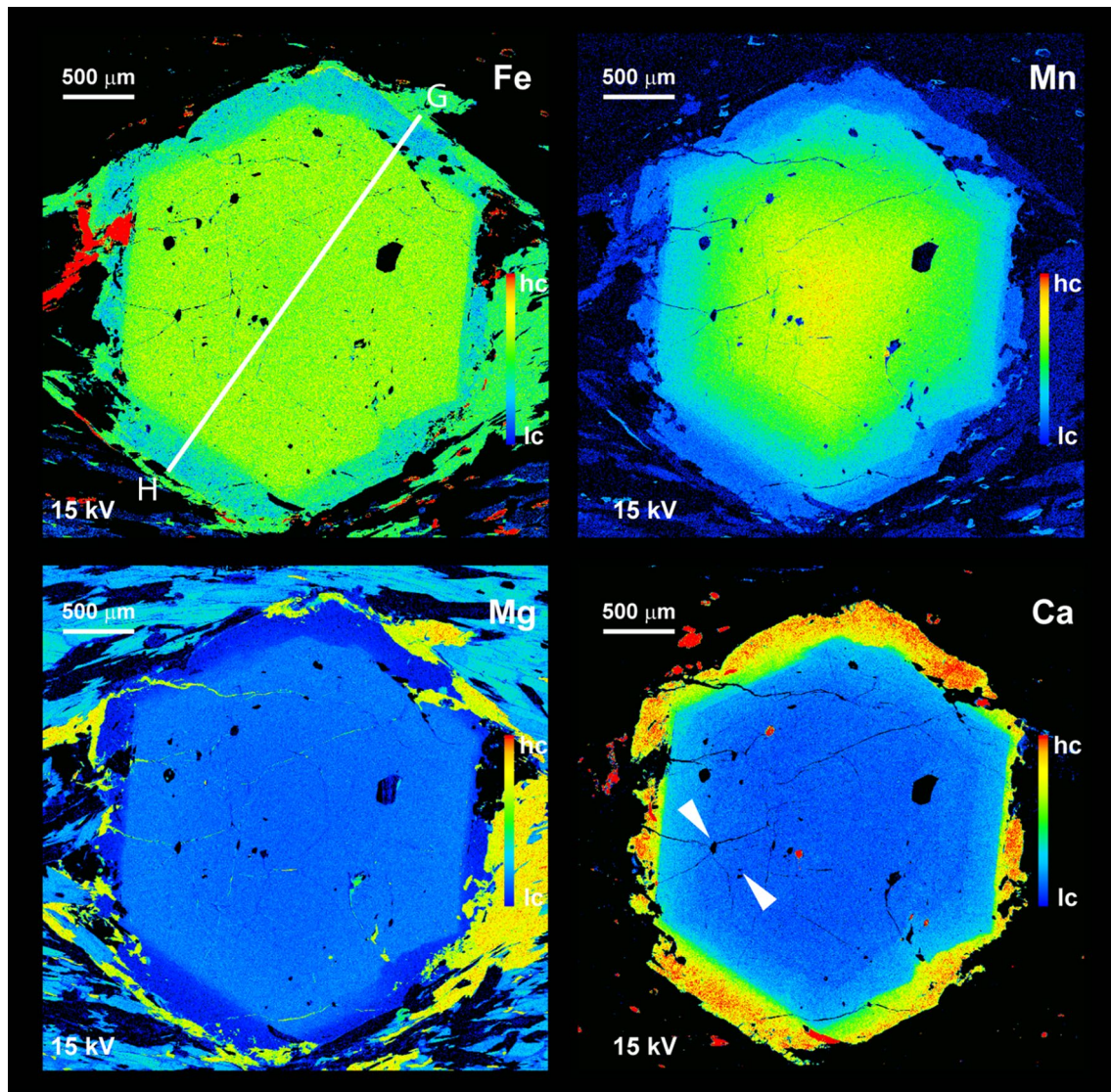


**Fig. 8** X-ray maps of a garnet from sample CH11. The white arrows in the Ca map indicate coesite and a polycrystalline aggregate of quartz included in garnet. The surface between garnet core and rim

is quite regular, suggesting no or limited dissolution of garnet core before the growth of garnet rim. By contrast, garnet rim is partially dissolved and replaced by chlorite

## Thermodynamic modelling

### *P–T* pseudosections

*P–T* mineral assemblage diagrams (pseudosections: Hensen 1971) and various key compositional and modal isopleths have been calculated for the studied coesite-bearing garnet–chloritoid micaschist sample (Figs. 10 and 11). The effects of fractionation of the zoned garnet as well as possible H<sub>2</sub>O undersaturation have been considered. The results have been compared with the observed mineral assemblages, inclusion suites and chemical zoning of garnet to infer the *P–T* path of the sample.

### Garnet cores

Two pseudosections were calculated in the system MnNCKFMASHTO in the *P–T* range 15–35 kbar and 400–600 °C. A pure H<sub>2</sub>O fluid phase was considered in excess. In the first pseudosection, calculated using the ICP–OES-measured whole-rock bulk composition, comparison of the measured garnet inner core composition (py = 6–7 mol%, grs = 5–6 mol%) and the corresponding isopleths suggests that the garnet inner core crystallised at ~ 470–500 °C ~ 25–27 kbar, in the g-ctd-jd-gl-law-mu-q-ru field, just below the quartz–coesite transition, compatible with the observed mineral assemblage. The occurrence of lawsonite in this field is consistent with the pseudomorphs

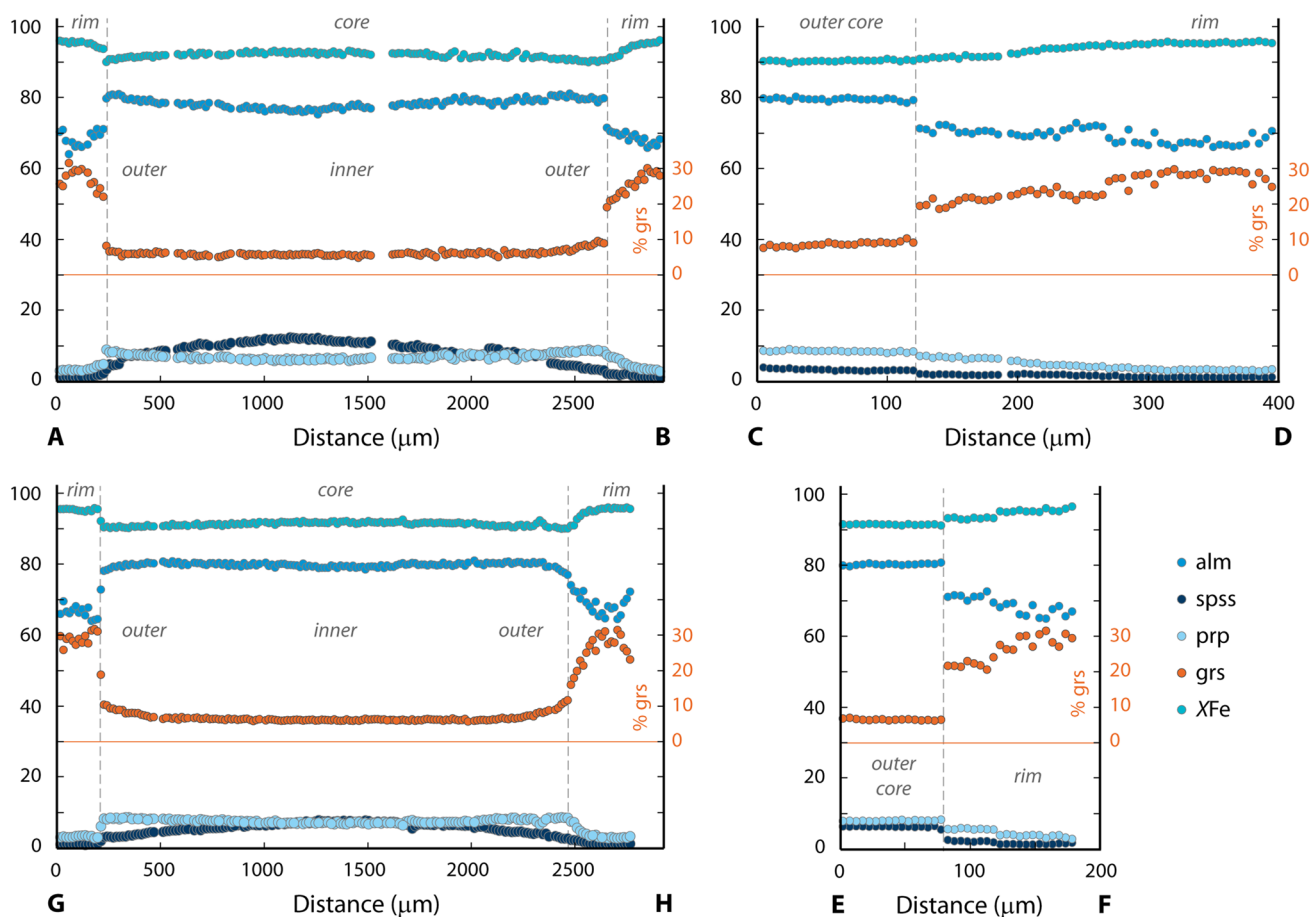


**Fig. 9** Compositional profiles of garnet for sample CH11. The position of the profiles is reported in Figs. 4 (lines A–B, C–D, E–F) and 5 (G–H)

observed. Calculated garnet and lawsonite modal abundances are less than 1 vol% and 1.5 vol%, respectively (Figs. 10, S10). The modelled content of spessartine is slightly higher than the observations, but decreases then with increasing temperature. The measured Si content in muscovite and  $X_{Mg}$  of chloritoid inclusions in the garnet inner core are consistent with the values (Si = 3.45–3.5 a.p.f.u.,  $X_{Mg}$  = 0.14–0.15, Fig. S11) modelled in the  $P$ – $T$  range inferred from the garnet inner core composition. The observed garnet zoning (continuous increase in pyrope, and decrease in spessartine and a roughly constant content of grossular) suggests subsequent garnet growth along a prograde up-pressure up-temperature  $P$ – $T$  path, subparallel to the grossular isopleths (grey arrow in Fig. 10c), that enters finally the stability field of coesite.

To estimate the conditions corresponding to the growth of the garnet outer core, a second pseudosection was calculated in the same  $P$ – $T$  range considering progressive garnet fractionation and subtracting the composition of garnet inner core from the measured bulk composition. Details on garnet fractionation are given in the Supporting Information. With respect to the first pseudosection,

garnet fractionation results in the displacement of the garnet-in line towards higher temperatures by ~30–40 °C, but the general topology as well as the position of the compositional isopleths are affected only marginally. Whereas the inner part of the outer core is characterised by the grossular content similar to that of the inner core (5–6 mol%), the outer part displays an increase in grossular (~6 → 9 mol%). This is compatible with a  $P$ – $T$  path that first follows the grossular isopleths and reaches maximum pressures in the coesite stability field at about 27–28 kbar 510–530 °C. Subsequently, the increase of the proportion of grossular indicates pressure decrease, while the temperature still slightly increases (allowing further crystallisation of garnet—see the position of the garnet mode isopleths in Fig. 10d). The crystallisation of the edge of the outer core corresponds to  $P$ – $T$  condition of ~25–26 kbar, 540 °C. The Si content of muscovite modelled in this field is of the order 3.40–3.45 a.p.f.u., consistent with the values measured in the studied sample. The measured  $X_{Mg}$  of chloritoid inclusions in the garnet outer core ( $X_{Mg}$  = 0.16–0.18, Fig. S11) are slightly lower than the values modelled in the  $P$ – $T$  range inferred from the garnet



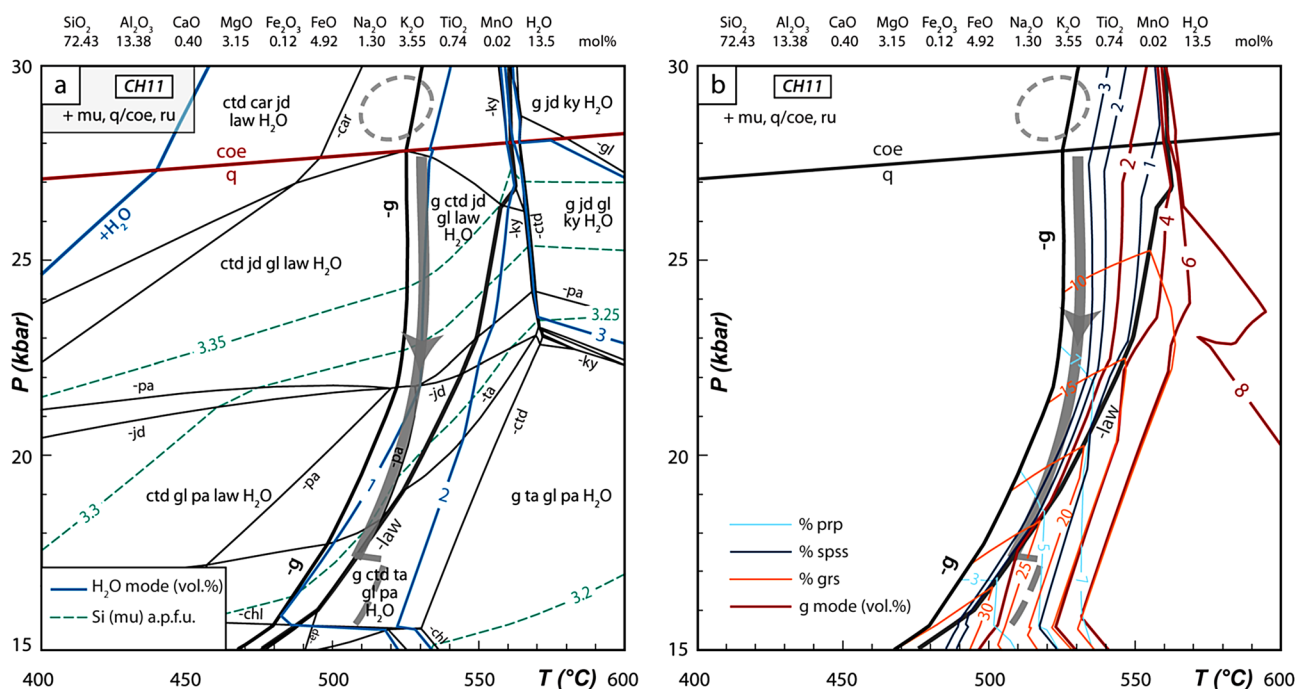


**Fig. 11**  $P$ – $T$  pseudosections calculated for the sample CH11, considering progressive garnet fractionation. **a**  $P$ – $T$  pseudosections calculated in the range 15–30 kbar and 400–600 °C, using a fixed amount of  $H_2O$  and the bulk-rock composition obtained by garnet core (inner

and outer) fractionation. **b** Garnet isopleths and its modal amount. The grey arrow in **(a)** and **(b)** is the inferred  $P$ – $T$  path followed during the growth of garnet rim. Colours for the garnet isopleths correspond to the ones used for the chemical profile in Fig. 9

account the corresponding isopleths in Fig. 10, this implies garnet growth at significantly lower pressures. Since decompression may lead to  $H_2O$  undersaturation (e.g., Le Bayon et al., 2006; Pitra et al., 2010; Manzotti et al., 2018), one pseudosection was calculated in the  $P$ – $T$  range 15–30 kbar 400–600 °C with a fixed amount of  $H_2O$ . This amount was determined so that the proportion of the fluid phase in the rock does not exceed 1 vol% (Thompson and Connolly 1990) at peak  $T$  (inferred from Fig. 10b). In the pseudosection calculated in the  $P$ – $T$  range 15–30 kbar, 400–600 °C the  $H_2O$ -saturation limit (blue line) has a positive slope and goes from 400 °C ~ 24 kbar, to 450 °C ~ 30 kbar and most of the diagram displays fluid-present assemblages (Fig. 11a). The trend of the isopleths for the grossular content in garnet is very sensitive to the presence of lawsonite (Fig. 11b). Whereas decompression or heating lead to an increase in grossular when lawsonite is present, they have the opposite effect in the lawsonite-absent domain. The trend of the isopleths of garnet mode (slightly positive slope) also shows that garnet can keep on crystallising upon decompression. The  $P$ – $T$  path (grey arrow in Figs. 11a,b), inferred from the zoning of the garnet rim, is characterised by strong decompression (from ~25 to ~17 kbar) accompanied by slight cooling (from ~540 to ~500 °C) in the lawsonite-present part of the diagram. This accounts for the strong increase in grossular and decrease in pyrope while ensuring continuous limited garnet growth ( $P$ – $T$  path continuously approaching the 2

vol% garnet mode isopleth). The final decrease in grossular (30 → 22 mol%), recorded in the outermost garnet rim, points to further decompression, possibly associated with slight heating (~15 °C) in the lawsonite-absent domain, to about 15 kbar, 500 to 515 °C. This is consistent with the final increase of pyrope observed locally in the outermost garnet rim, the sub-isothermal trend of the isopleths of pyrope in the field g-ctd-gl-ta-pa-mu-ru-q, and the negative slope of both grossular and pyrope isopleths in the chlorite-bearing fields (Fig. 11b). Although this temperature increase is quantitatively negligible and well below the uncertainties on the absolute values estimated, it does have an indubitable qualitative significance.

The trend of the isopleths of chloritoid mode (Fig. S12) indicates that chloritoid is consumed during decompression along the  $P$ – $T$  path (grey arrow in Fig. 11a, b), inferred from the zoning of the garnet rim. The growth of the thin rim in chloritoid ( $X_{Mg} = 0.12$ – $0.09$ ) marking the main foliation is modelled at ~16 kbar and is associated with a decrease in temperature (Fig. S12).

## Discussion

Since 1984, Brossasco-Isasca was the only *UHP* unit recognized in the Dora-Maira Massif. Its peculiarity inspired a large number of studies and attracted hundreds

of geologists in the field (up to the woeful point that today nothing is left of some of its most spectacular outcrops). Key distinctive features of the Brossasco-Isasca Unit are (i) the pyrope–kyanite–coesite whiteschists, derived from hydrothermally altered granitoids (Ferrando et al. 2009; Gauthiez-Putallaz et al. 2016), (ii) garnet–kyanite–jadeite assemblages in metapelites, with rare relicts of a pre-Alpine garnet, (iii) *UHP* assemblages in mafic boudins and interbedded marbles in the metapelites, and (iv) the scarcity of *UHP* relicts in the granitic orthogneisses (Compagnoni and Rolfo 2003 and refs therein).

Thirty-eight years after the identification of the Brossasco-Isasca Unit (Chopin 1984), we have discovered a new, colder *UHP* unit, the Chasteiran Unit, in the less explored northern Dora-Maira Massif (Fig. 2). Pending further exploration, we adopted the name Chasteiran Unit for the distinctive garnet–chloritoid layer characterized by its structural position in the immediate hangingwall of the Pinerolo Unit, and by the occurrence—at least in one locality, namely, the Chasteiran church—of coesite. The true extent of the *UHP* metamorphism will be defined in the future using further petrological studies aimed at discovering other examples of coesite inclusions preserved in garnet cores, and/or garnet core composition indicative of *UHP* conditions, for the appropriate bulk chemistry. In a few cases, we found strongly foliated augengneisses that may be part of the Chasteiran Unit, although their exact relationship with the garnet–chloritoid micaschist needs further clarification. Given the poor outcrop conditions in the forest, we have not been able to find an exposed contact between the two lithologies. The age of the protoliths of the graphite-rich, garnet–chloritoid micaschist from the Chasteiran Unit is uncertain. The most straightforward hypothesis is to derive them from the (graptolite-bearing) black shales so common in the Silurian successions found throughout the Palaeozoic of Western and Central Europe (e.g., Kříž et al. 2003; Corradini et al. 2009). This would be consistent with (i) the much higher amount of graphite in the Chasteiran micaschist, compared to other garnet–chloritoid micaschists from the Dora-Maira Massif and (ii) the lack of interbedded quartzite and/or marble within the graphite-rich micaschist, suggesting an episode of anoxic sedimentation during a rather large time interval. Last, we also envisaged that the protolith of the distinctive garnet–chloritoid layer may have been deposited in a Carboniferous basin, similar to the Pinerolo Unit, but this hypothesis faces several difficulties, e.g., the lack of meta-conglomerates or meta-sandstones. To the best of our present knowledge, the Chasteiran Unit is only a few tens of metres thick and consists of graphite-rich, garnet–chloritoid micaschist.

## The garnet record

Garnet is scarce, concentrated in mica-rich domains, and is optically and chemically zoned. Cores are colourless and characterised by a prograde growth zoning with a decrease in spessartine and increase in pyrope. Thermodynamic modelling indicates that garnet inner cores and outer cores crystallised at  $\sim 470\text{--}500\text{ }^{\circ}\text{C}$   $\sim 25\text{--}27\text{ kbar}$  and  $\sim 510\text{--}530\text{ }^{\circ}\text{C}$   $\sim 27\text{--}28\text{ kbar}$ , respectively. Garnet outer cores crystallised in the coesite stability field as also indicated by pristine as well as partly pseudomorphed coesite inclusions identified in this domain.

Garnet rims are light pink in colour and display a decrease in pyrope and a continuous and significant increase in grossular followed by a slight decrease in this end-member. Petrographic and microstructural observations indicate no other optical discontinuity than a colour change between garnet outer cores and rims, suggesting no or very limited dissolution and resorption of garnet cores before the growth of garnet rims. A break in chemical composition at the interface between garnet outer cores and garnet rims (see chemical profiles of Fig. 9) is observed and this resembles those found in multistage garnet associated with two orogenic cycles (e.g., Karabinos 1984; Ganne et al. 2003; Gaidies et al. 2006; Le Bayon et al. 2006; Feenstra et al. 2007; Sandmann et al. 2014; Giuntoli et al. 2018; Cruciani et al. 2021; Klug and Froitzheim 2021; Nosenzo et al. 2022) or in metamorphic garnet overgrowths on detrital grains (Yardley et al. 1996; Manzotti and Ballèvre 2013). The chemistry of garnet core may be marginally compatible with its growth at low  $P$  in a biotite–talc–amphibole–ilmenite with plagioclase or paragonite assemblage. However, this hypothesis can be excluded given the presence of chloritoid (not stable below 14kbar) and rutile inclusions in garnet inner as well as outer cores (see Fig. S13). The strongest evidence against the hypothesis of a pre-Alpine garnet core is that coesite inclusions do occur in the garnet outer cores, not in the rims. For the latter, thermodynamic modelling indicates that the  $P$ – $T$  evolution occurred under fluid-present conditions and that garnet rims crystallised during decompression between  $\sim 25\text{--}15\text{ kbar}$   $\sim 540\text{--}500\text{ }^{\circ}\text{C}$ .

## Strain history of the studied sample

Garnet porphyroblasts are excellent recorders of the strain history with respect to the metamorphic history, and the studied sample is no exception to this rule. Four metamorphic stages have been distinguished (Fig. 3). Stages 1 and 2 occurred during growth of garnet cores, into which the inclusions do not display a preferential shape orientation. It is, therefore, difficult to assess the strain history during this time period. Inclusions in garnet rims (stage 3) occasionally display a preferential orientation, indicating that garnet

overgrew a foliation ( $S_1$ ) during the growth of the garnet rim. This early foliation is also recorded by isoclinal, intrafolial folds observed in the muscovite- and chloritoid-rich layers. The main foliation ( $S_2$ ) is a composite foliation, resulting from the folding and flattening of an earlier fabric ( $S_1$ , Fig. S4a), defined by the shape preferred orientation of muscovite, chloritoid and rutile, overgrown during stage 4 by a new generation of chloritoid (i.e., the rims with a lower  $X_{Mg}$ ), chlorite (also partly dissolving garnet rims), and ilmenite.

Several observations may help to understand the rheological behaviour of garnet during this multistage history. In one instance, the occurrence of thin and discontinuous domains consisting of garnet rim compositions around dissected garnet fragments indicates that garnet fractures developed after the growth of garnet core (stages 1 and 2) and before the crystallization of garnet rim (stage 3), between 28 and 25 kbar. This texture indicates that some garnet crystals may display brittle deformation in a ductilely deforming matrix during decompression at high pressure. In this case, the timing of garnet fracturation is unambiguously defined because of its relationships with the growth zoning. Other fractures, filled with chlorite, have developed in most garnet grains during stage 4.

With respect to the regional geology, the strain history of the sample would be compatible with a model, where the continental crust does not deform pervasively during the burial stage (stages 1 and 2), and where the foliation initiation took place at the beginning of the exhumation history (stage 3). This may be related to a rigid behaviour of the downgoing slab (with metamorphic reactions proceeding from the quartz into the coesite stability fields), or to a significant strain partitioning, leaving some undeformed pods, such as the famous Brossasco granite (e.g., Biino and Compagnoni 1992; Lenze and Stöckhert 2007). The onset of the ductile deformation would then record the detachment of the Chasteiran Unit from the downgoing slab, and ultimately its emplacement over the Pinerolo Unit. Consequently, the main regional foliation, which is parallel to the main tectonic boundary with the underlying Pinerolo Unit (see Fig. 2), developed during exhumation of the coesite-bearing Chasteiran Unit, most probably during thrusting of the Chasteiran Unit over the Pinerolo Unit. A similar history has been inferred for the *UHP* Brossasco-Isasca Unit (Henry et al. 1993; Avigad et al. 2003).

### Lack of evidence for polycyclic garnets in the Chasteiran Unit

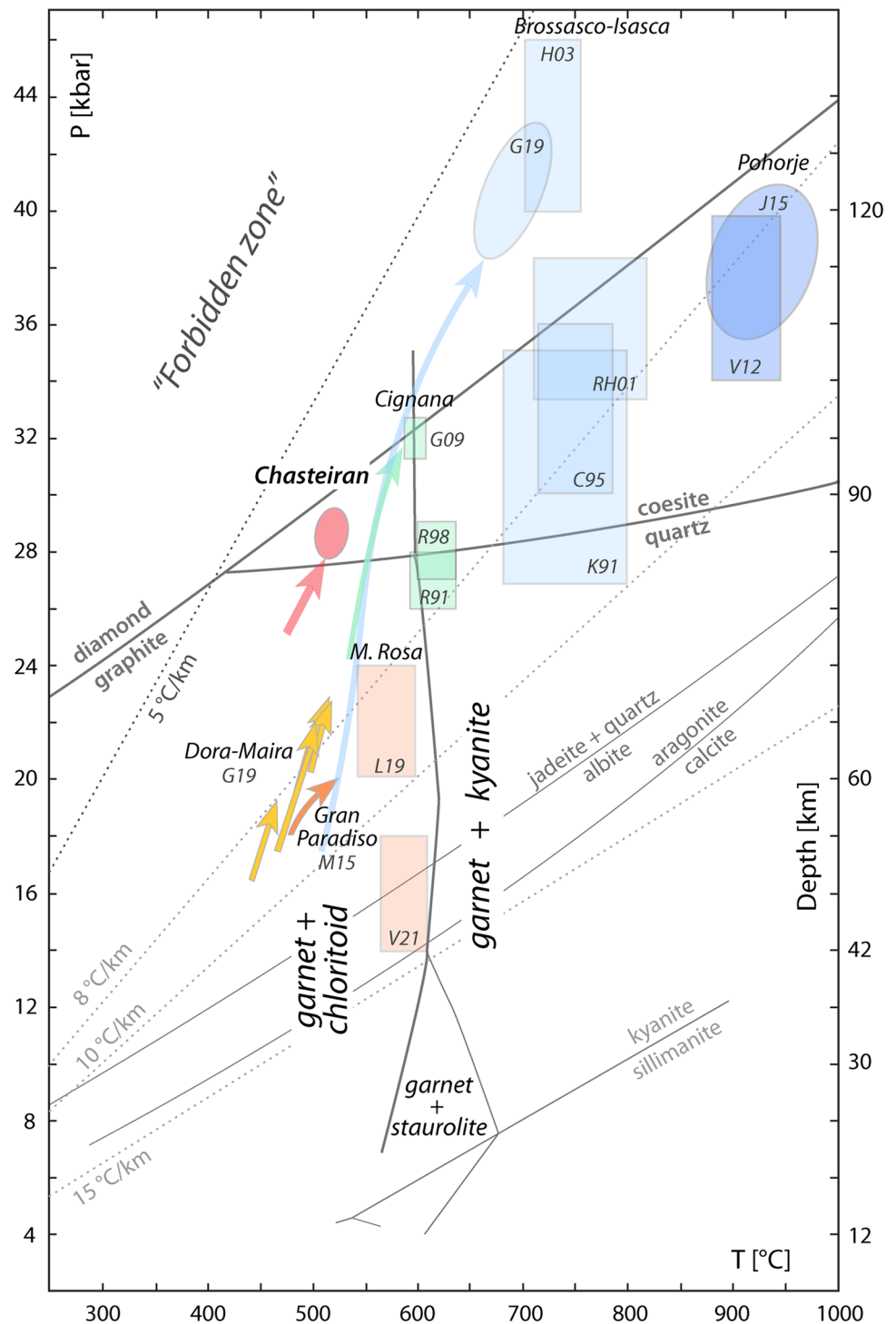
Polycyclic garnets associated with two orogenic cycles are commonly observed in the micaschist of the *HP* Muret Unit (Nosenzo et al. 2022 and refs therein). However, we have not been able to identify multistage garnets in the *UHP* Chasteiran Unit. Garnet–chloritoid micaschist similar to

the one constituting the Chasteiran Unit has been described in other units from the southern Dora-Maira Massif, such as the *UHP* Brossasco-Isasca and the *HP* Rocca-Solei, San Chiaffredo and Ricordone Units (e.g., Henry et al. 1993; Groppo et al. 2019). These units are considered as portions of the pre-Alpine continental crust that experienced Variscan amphibolite-facies metamorphism (e.g., Matsumoto and Hirajima 2000; Compagnoni and Rolfo 2003) as suggested by garnet and staurolite relicts. However, in the Chasteiran Unit staurolite relicts are not observed. Therefore, if the Chasteiran Unit is also a slice of Palaeozoic basement (and thus polycyclic), the absence of multistage garnets may be attributed to a complete rock re-equilibration occurring during the Alpine history or to a heterogeneous distribution of polycyclic garnet inside the unit. Alternatively, a relatively low-grade pre-Alpine metamorphism (at lower  $P$ – $T$  conditions than the garnet–staurolite stability field) may explain the absence of multistage garnets. Such a low-grade pre-Alpine metamorphism characterizes for example the Palaeozoic basement of part of the Vanoise Massif (Briançonnais domain; for a summary and a discussion see Bergomi et al. 2017; Ballèvre et al. 2018). Finally, we cannot a priori exclude on a petrological basis the hypothesis that the Chasteiran Unit is monocyclic and made of Mesozoic sediments. Mesozoic continental sediments in the Alps are by far dominated by meta-limestones and meta-marls, i.e., calcite-bearing schists (e.g., Michard et al. 2022). Calcium-poor or calcium-absent lithologies derived from pelitic schists developed during the anoxic events, mainly of mid-Cretaceous age. These considerations would narrow the temporal range for the deposition of the protolith of the studied meta-sediments, and would require an additional (tectonic?) explanation for the lack of any other Mesozoic sediment. As a whole, this latter hypothesis seems very unlikely.

### Fe-rich chloritoid stability at *UHP* conditions

A distinctive characteristic of the Chasteiran Unit, compared to the Brossasco-Isasca Unit, is the widespread occurrence of chloritoid in the coesite-bearing micaschist. Field data and thermodynamic modelling show that, in normal pelitic composition (i.e., rather aluminous with  $X_{Mg}$  ratios in the range of 0.20–0.50), chloritoid stability field is bounded towards higher  $T$  by staurolite-producing reactions (at  $P$  lower than  $\sim 14$  kbar), and by garnet–kyanite producing reactions at  $P$  higher than  $\sim 14$  kbar (Fig. 12). A narrow subisothermal band (c. 600–650 °C) with garnet–chloritoid–kyanite assemblages separates a low- $T$  garnet–chloritoid domain from the high- $T$  garnet–kyanite assemblages (e.g., Smye et al. 2010). The question, therefore, arises, in the studied sample, whether chloritoid was stable throughout the metamorphic history, or whether its stability field has been exceeded at peak

**Fig. 12**  $P$ – $T$  diagram displaying the peak  $P$ – $T$  conditions reached by the UHP Chasteiran, Cignana, Brossasco-Isasca, and Pohorje Units. The peak  $P$ – $T$  conditions reached by the HP Gran Paradiso Unit are also reported for comparison. The univariant reactions depicted in this figure have been calculated using THERMOCALC. Selection of  $P$ – $T$  conditions estimated for the different Units are from: (i) Gran Paradiso Unit: M15—Manzotti et al. 2015; (ii) Lago di Cignana Unit: R91—Reinecke 1991, R98—Reinecke 1998, G09—Groppo et al. 2009; (iii) Brossasco-Isasca Unit: K91—Kienast et al. 1991, C95—Compagnoni et al. 1995, RH01—Rubatto and Hermann 2001, H03—Hermann 2003; G19—Groppo et al. 2019; (iv) Dora-Maira Units: G19—Groppo et al. 2019; (v) Monte Rosa: L19—Luisier et al. 2019; V21—Vaughan-Hammon et al. 2021; (vi) Pohorje: V12—Vrabc et al. 2012; J15—Janák et al. 2015. For comparison, we chose to show only the prograde  $P$ – $T$  paths calculated by modelling the garnet growth zonings



(UHP) conditions, in which case chloritoid may result of a retrograde development during decreasing  $T$  at decreasing  $P$  and the Chasteiran micaschist could then be a northern equivalent of the Brossasco-Isasca rocks, strongly sheared and retrogressed in the chloritoid stability field. This question is not just a petrological issue, because it has significant tectonic implications.

There are three lines of evidence against such a hypothesis. First, textural observations indicate that chloritoid was present in the studied rock during its entire life cycle (Fig. 3). Chloritoid is found included in garnet inner cores (stage 1, Figs. 3 and 4) as well as outer cores (where coesite is also found, stage 2), and defines the foliation synchronous of the growth of garnet rims (stage 3). Moreover, there is a

systematic change in chemistry of chloritoid with chloritoid associated with stage 1 being less Mg-rich and more Mn-rich than chloritoid stable during stages 2 and 3, consistent with the evolution of garnet composition (Figs. 3, S6 and S14). The same holds for the rims of the matrix chloritoid that grew during stage 4.

Second, thermodynamic modelling of garnet composition predicts its stability in a large part of the  $P$ – $T$  space, in the chloritoid-bearing as well as chloritoid-absent assemblages. However, a garnet with the observed chemical composition is only stable in chloritoid-bearing assemblages, in agreement with textural observations.

Third, RSCM data ( $T$  of  $483 \pm 17$  °C) validate the ‘cold’ nature of the Chasteiran *UHP* metamorphism. Given the absolute uncertainties associated with the RSCM method (50 °C or 25 °C, according to Beyssac et al. 2002 and Beyssac et al. 2019, respectively), such values are in agreement with those derived from the pseudosection modelling. These  $T$  conditions are  $\sim 200$  °C lower than the one experienced by the Brossasco-Isasca Unit (e.g., Chopin et al. 1991; Compagnoni et al. 1995; Beyssac et al. 2002; Coggon and Holland 2002; Compagnoni and Rolfo 2003; Hermann 2003; Castelli et al. 2007; Ferrando et al. 2017; Campomenosi et al. 2021). These higher  $T$  estimates for the Brossasco-Isasca Unit are consistent with the observation that chloritoid (and staurolite) may have been present during the prograde history of the Brossasco-Isasca micaschists, but the *UHP* equilibration took place outside their stability field, when kyanite was an essential component of the mineral assemblage.

### A new, colder, *UHP* Unit in the Alpine belt

We are, therefore, quite confident that the Chasteiran Unit equilibrated at *UHP* conditions in the chloritoid stability field and, therefore, represents a distinct, colder, *UHP* unit with respect to the Brossasco-Isasca Unit. It is, in fact, the coldest reported *UHP* unit in the Alpine belt (Fig. 12), given the  $P$ – $T$  values estimated for the Pohorje Mountains (Vrabec et al. 2012; Janák et al. 2015), and the Lago di Cignana (Reinecke 1991, 1998; Groppo et al. 2009). The latter may have been equilibrated close to the upper boundary of the chloritoid stability field. Outside the Alpine belt, chloritoid-bearing *UHP* rocks are extremely rare (see compilations in Coleman and Wang 1995; Carswell and Compagnoni 2003; Gilotti 2013). The presence of chloritoid-bearing *UHP* rocks in the Western Alps has been, however, suspected following the discovery of a Roman quern-stone made of a garnet–chloritoid talcschist, with relict coesite observed as inclusions in garnet (Groppo et al. 2016). Our discovery does not provide an answer about the location of the rock used as a primary material for the quern-stone, because this lithology is very different from the ones constituting the Chasteiran Unit. A survey of the worldwide occurrences of

coesite-bearing rocks indicates that, other than the occurrence described here, the only coesite- and chloritoid-bearing rocks are found in the Tian Shan in Kirghizistan (Tagiri and Bakirov 1990; Orozbaev et al. 2015) and neighbouring Xinjiang (Zhang et al. 2003; Lü et al. 2008, 2009, 2014).

## Conclusions and perspectives

This study leads to the following conclusions:

1. We identified a new *UHP* unit, named Chasteiran Unit, in the northern Dora-Maira Massif. It is only a few tens of metres thick and discontinuously exposed above the contact with the lower grade Pinerolo Unit. The Chasteiran Unit is the fourth and the coldest Alpine *UHP* unit known so far in the entire Alpine belt.
2. Pristine and relict coesite occur in garnet outer cores together with chloritoid inclusions suggesting that the Chasteiran Unit equilibrated at *UHP* conditions in the chloritoid stability field. Thermodynamic modelling indicates peak  $P$ – $T$  conditions at 27–28 kbar, 510–530 °C, consistent within uncertainty with the RSCM estimates. Amongst the other *UHP* terranes known around the world, these conditions are only recorded by some *UHP* rocks found in the Tian Shan.
3. Identification of this new, colder, *UHP* unit has been possible through a systematic, detailed study of minute (at most 20  $\mu\text{m}$  long) coesite inclusions, the largest of which displaying palisade quartz, the smallest being pristine (no partial pseudomorph, no radial cracks). Our discovery shows that some *UHP* rocks may have escaped the attention of the petrologists, and that *UHP* units may be more common in low-temperature rocks (i.e., in garnet–chloritoid bearing assemblages) than previously thought.
4. From a tectonic perspective, the discovery of coesite-bearing rocks in the northern Dora-Maira Massif, in the immediate hangingwall of the Sanfront–Pinerolo Unit, implies that the *UHP* rocks from the southern (Brossasco-Isasca) and northern (Chasteiran) Dora-Maira Massif occupy the same structural position, unambiguously displaying thrusting of higher over lower  $P$  rocks. However, the two *UHP* units (Brossasco-Isasca and Chasteiran) record different peak  $P$ – $T$  conditions (30–40 kbar  $\sim$  700–750 °C and 27–28 kbar 510–530 °C, respectively), indicating that they represent different slices detached from the downgoing slab.

Further investigations are now underway about the Chasteiran Unit, to better characterize its geometry (requiring further mapping in a densely forested area), and to determine the timing and rate of its burial and exhumation. These

data integrated with the tectonic evolution are critical to resolve the debate regarding collisional processes and exhumation mechanisms. Specifically, this will allow us to understand when and how thin tectonic *UHP* units were sliced off, this process being a characteristic of the Alpine belt along its entire length (i.e., from Dora-Maira to Pohorje), in contrast with other belts, where huge and thick *UHP* domains have been exhumed (e.g., Kylander-Clark et al. 2012).

**Supplementary Information** The online version contains supplementary material available at <https://doi.org/10.1007/s00410-022-01923-8>.

**Acknowledgements** This study was financially supported by a Starting Grant from Stockholm University to Paola Manzotti (Fund 4615701). Jessica Langlade (Micosonde Ouest, Brest, France) and Martin Robyr (University of Lausanne, Switzerland) are thanked for assistance during EPMA data acquisition. Discussions in the field in September 2021 with Stefan Schmid were strongly appreciated. We thank Christian Chopin and Guillaume Bonnet for their detailed constructive reviews. The editorial work of Hans Keppler has been highly appreciated.

**Funding** Open access funding provided by Stockholm University.

**Open Access** This article is licensed under a Creative Commons Attribution 4.0 International License, which permits use, sharing, adaptation, distribution and reproduction in any medium or format, as long as you give appropriate credit to the original author(s) and the source, provide a link to the Creative Commons licence, and indicate if changes were made. The images or other third party material in this article are included in the article's Creative Commons licence, unless indicated otherwise in a credit line to the material. If material is not included in the article's Creative Commons licence and your intended use is not permitted by statutory regulation or exceeds the permitted use, you will need to obtain permission directly from the copyright holder. To view a copy of this licence, visit <http://creativecommons.org/licenses/by/4.0/>.

## References

- Avigad D, Chopin C, Le Bayon R (2003) Thrusting and extension in the southern Dora-Maira ultra-high pressure Massif (Western Alps): view from below the coesite-bearing Unit. *J Geol* 111:57–70
- Ballèvre M, Manzotti P, Dal Piaz GV (2018) Pre-Alpine (Variscan) inheritance: a key for the location of the future Valais Basin (Western Alps). *Tectonics* 37:786–817
- Ballèvre M, Camonin A, Manzotti P, Poujol M (2020) A step towards unravelling the paleogeographic attribution of pre-Mesozoic basement complexes in the Western Alps based on U-Pb geochronology of Permian magmatism. *Swiss J Geosci* 113:12
- Bergomi MA, Dal Piaz GV, Malusà MG, Monopoli B, Tunesi A (2017) The Grand St Bernard-Briançonnais nappe system and the Paleozoic inheritance of the Western Alps unraveled by zircon U-Pb dating. *Tectonics* 36:2950–2972
- Beysac O, Goffé B, Chopin C, Rouzaud JN (2002) Raman spectra of carbonaceous material in metasediments: a new geothermometer. *J Metamorph Geol* 20:859–871
- Beysac O, Pattison DRM, Bourdelle F (2019) Contrasting degrees of recrystallization of carbonaceous material in the Nelson aureole, British Columbia and Ballachulish aureole, Scotland, with implications for thermometry based on Raman spectroscopy of carbonaceous material. *J Metamorph Geol* 37:71–95
- Biino GG, Compagnoni R (1992) Very-high pressure metamorphism of the Brossasco coronate metagranite, southern Dora Maira Massif, Western Alps. *Schweiz Mineral Petrogr Mitt* 72:347–363
- Bonnet G, Chopin C, Locatelli M, Kylander-Clark ARC, Hacker BR (2022) Protracted subduction of the European hyperextended margin revealed by rutile U-Pb geochronology across the Dora-Maira Massif (Western Alps). *Tectonics* 41:e2022TC007170
- Borghi A, Cadoppi P, Porro A, Sacchi R, Sandrone R (1984) Osservazioni geologiche nella Valle Germanasca e nella media Val Chisone (Alpi Cozie). *Boll Mus Reg Sci Nat Torino* 2:503–530
- Borghi A, Cadoppi P, Porro A, Sacchi R (1985) Metamorphism in the north part of the Dora-Maira Massif (Cottian Alps). *Boll Mus Reg Sci Nat Torino* 3:369–380
- Borghi A, Sandrone A (1990) Structural and metamorphic constraints to the evolution of a NW sector of Dora-Maira Massif (Western Alps). *Mem Soc Geol It* 45:135–141
- Borghi A, Compagnoni R, Sandrone R (1996) Composite P-T paths in the Internal Penninic massifs of the Western Alps: petrological constraints to their thermomechanical evolution. *Eclogae Geol Helv* 89:345–367
- Bousquet R, Oberhänsli R, Schmid SM, Berger A, Wiederkehr M, Robert C, Möller A, Rosenberg C, Zeilinger G, Molli G, Koller F (2012) Metamorphic framework of the Alps. Commission for the geological map of the world; subcommission for magmatic and metamorphic maps. IUGS and IUGG, Paris. <http://www.ccgmap.org>
- Boyer H, Smith DC, Chopin C, Lasnier B (1985) Raman microprobe (RMP) determinations of natural and synthetic coesite. *Phys Chem Miner* 12:45–48
- Bussy F, Cadoppi P (1996) U-Pb dating of granitoids from the Dora-Maira massif (western Italian Alps). *Schweiz Mineral Petrogr Mitt* 76:217–233
- Cadoppi P, Castelletto M, Sacchi R, Baggio P, Carraro F, Giraud V, Bellardone G (2002) Carta geologica d'Italia alla scala 1:50.000, Foglio 154 Susa. *Geol Surv It*
- Cadoppi P, Camanni G, Balestro G, Perrone G (2016) Geology of the Fontane talc mineralization (Germanasca valley, Italian Western Alps). *J Maps* 12:1170–1177
- Campomenosi N, Scambelluri M, Angel RJ, Hermann J, Mazzucchelli ML, Mihailova B, Piccoli F, Alvaro M (2021) Using the elastic properties of zircon-garnet host-inclusion pairs for thermobarometry of the ultrahigh-pressure Dora-Maira whiteschists: problems and perspectives. *Contrib Mineral Petrol* 176:36
- Carignan J, Hild P, Mevelle G, Morel J, Yeghicheyan D (2001) Routine analyses of trace elements in geological samples using flow injection and low pressure on-line liquid chromatography coupled to ICP-MS: a study of geochemical reference materials, BR, DRN, UB-N, AN-G and GH. *Geostandard Newslett* 25:187–198
- Carraro F, Cadoppi P, Castelletto M, Sacchi R, Baggio P, Giraud V, Bellardone G (2002) Note illustrative della carta geologica d'Italia alla scala 1:50.000, Foglio 154 Susa. Servizio Geologico d'Italia
- Carswell DA, Compagnoni R (eds) (2003) Ultrahigh Pressure metamorphism. European Mineralogical Union Notes in Mineralogy, vol 5
- Castelli D, Rolfo F, Groppo C, Compagnoni R (2007) Impure marbles from the UHP Brossasco-Isasca Unit (Dora-Maira Massif, Western Alps): evidence for Alpine equilibration in the diamond stability field and evaluation of the X(CO<sub>2</sub>) fluid evolution. *J Metamorph Geol* 25:587–603
- Chopin C (1984) Coesite and pure pyrope in high-grade blueschists of the Western Alps: a first record and some consequences. *Contrib Mineral Petrol* 86:107–118
- Chopin C, Schertl H-P (1999) The UHP Unit in the Dora Maira Massif, Western Alps. *Int Geol Rev* 41:765–780

- Chopin C (2003) Ultrahigh-pressure metamorphism: tracing continental crust into the mantle. *Earth Planet Sci Lett* 212:1–14
- Chopin C, Henry C, Michard A (1991) Geology and petrology of the coesite-bearing terrain, Dora Maira massif, Western Alps. *Eur J Mineral* 3:263–291
- Coggon R, Holland TJB (2002) Mixing properties of phengitic micas and revised garnet-phengite thermobarometers. *J Metamorph Geol* 20:683–696
- Coleman RG, Wang X (eds) (1995) Ultrahigh pressure metamorphism. Cambridge University Press, Cambridge, p 528p
- Compagnoni R (1977) The Sesia-Lanzo Zone: high pressure-low temperature metamorphism in the Austroalpine continental margin. *Rend Soc Ital Min Petrol* 33:335–378
- Compagnoni R, Hirajima T (2001) Superzoned garnets in the coesite-bearing Brossasco-Isasca Unit, Dora-Maira massif, Western Alps, and the origin of the whiteschist. *Lithos* 57:219–236
- Compagnoni R, Rolfo F (2003) UHPM units in the Western Alps. *EMU Notes Mineral* 5:13–49
- Compagnoni R, Hirajima T, Chopin C (1995) Ultra-high-pressure metamorphic rocks in the Western Alps. In: Coleman RG, Wang X (eds) Ultrahigh pressure metamorphism. Cambridge University Press, Cambridge, pp 206–243
- Compagnoni R, Rolfo F, Groppo C, Hirajima TR (2012) Geological map of the ultra-high pressure Brossasco-Isasca unit (Western Alps, Italy). *J Maps* 8:465–472
- Corradini C, Ferretti A, Storch P (2009) The Silurian of Sardinia. *Rend Soc Pal It* 3:1–167
- Cruciani G, Franceschelli M, Massonne H-J, Musumeci G (2021) Evidence of two metamorphic cycles preserved in garnet from felsic granulite in the southern Variscan belt of Corsica. *France Lithos* 380–381:105919
- de Capitani C, Brown TH (1987) The computation of chemical equilibrium in complex systems containing non-ideal solutions. *Geochim Cosmochim Acta* 51:2639–2652
- de Capitani C, Petrakakis K (2010) The computation of equilibrium assemblage diagrams with Theriak/Domino software. *Amer Miner* 95:1006–1016
- Feenstra A, Petrakakis K, Rhede D (2007) Variscan relicts in Alpine high-P pelitic rocks from Samos (Greece): evidence from multi-stage garnet and its included minerals. *J Metamorph Geol* 25:1011–1033
- Ferrando S, Frezzotti ML, Petrelli M, Compagnoni R (2009) Metasomatism of continental crust during subduction: the UHP whiteschists from the Southern Dora-Maira Massif (Italian Western Alps). *J Metamorph Geol* 27:739–756
- Ferrando S, Groppo C, Frezzotti ML, Castelli D, Proyer A (2017) Dissolving dolomite in a stable UHP mineral assemblage: evidence from Cal-Dol marbles of the Dora-Maira Massif (Italian Western Alps). *Am Mineral* 102:42–60
- Gaidies F, Abart R, De Capitani C, Schuster R, Connolly AD, Reusser E (2006) Characterization of polymetamorphism in the Austroalpine basement east of the Tauern Window using garnet isopleth thermobarometry. *J Metamorph Geol* 24:451–475
- Ganne J, Bussy F, Vidal O (2003) Multi-stage garnet in the internal Briançonnais basement (Ambin Massif, Savoy): new petrological constraints on the blueschist-facies metamorphism in the Western Alps and tectonic implications. *J Petrol* 44:1281–1308
- Gauthiez-Putallaz L, Rubatto D, Hermann J (2016) Dating prograde fluid pulses during subduction by in situ U-Pb and oxygen isotope analysis. *Contrib Mineral Petrol* 171:1–20
- Gillet P, Le Cléac’h A, Madon M (1990) High-temperature Raman spectroscopy of SiO<sub>2</sub> and GeO<sub>2</sub> polymorphs: anharmonicity and thermodynamic properties at high temperatures. *J Geophys Res* 95:21635–21655
- Gilotti JA (2013) The realm of ultrahigh-pressure metamorphism. *Elements* 9:255–260
- Giuntoli F, Lanari P, Engi M (2018) Deeply subducted continental fragments—part 1: fracturing, dissolution-precipitation, and diffusion processes recorded by garnet textures of the central Sesia Zone (western Italian Alps). *Solid Earth* 9:167–189
- Groppo C, Beltrando M, Compagnoni R (2009) The P-T path of the ultra-high pressure Lago Di Cignana and adjoining high-pressure meta-ophiolitic units: insights into the evolution of the subducting Tethyan slab. *J Metamorph Geol* 27:207–231
- Groppo C, Ferrando S, Castelli D, Elia D, Meirano V, Facchinetti L (2016) A possible new UHP unit in the Western Alps as revealed by ancient Roman quern-stones from Costigliole Saluzzo, Italy. *Eur J Mineral* 28:1215–1232
- Groppo C, Ferrando S, Gilio M, Botta S, Nosenzo F, Balestro G, Festa A, Rolfo F (2019) What’s in the sandwich? New P-T constraints for the (U)HP nappe stack of southern Dora-Maira Massif (Western Alps). *Eur J Mineral* 31:665–683
- Handy MR, Schmid SM, Bousquet R, Kissling E, Bernoulli D (2010) Reconciling plate-tectonic reconstructions of Alpine Tethys with the geological–geophysical record of spreading and subduction in the Alps. *Earth-Sci Rev* 102:121–158
- Hemley RJ (1987) Pressure dependence of Raman spectra of SiO<sub>2</sub> polymorphs:  $\alpha$ -quartz, coesite, and stishovite. *Geophys Monogr Ser* 39:347–359
- Henry C, Michard A, Chopin C (1993) Geometry and structural evolution of ultra-high-pressure and high-pressure rocks from the Dora-Maira massif, Western Alps, Italy. *J Struct Geol* 8:965–981
- Hensen BJ (1971) Theoretical phase relations involving garnet and cordierite in the system MgO–FeO–Al<sub>2</sub>O<sub>3</sub>–SiO<sub>2</sub>. *Contrib Mineral Petrol* 33:191–214
- Hermann J (2003) Experimental evidence for diamond-facies metamorphism in the Dora-Maira massif. *Lithos* 70:163–182
- Holland TJB, Powell R (1998) An internally consistent thermodynamic data set for phases of petrological interest. *J Metamorph Geol* 16:309–343
- Holland TJB, Powell R (2011) An improved and extended internally consistent thermodynamic dataset for phases of petrological interest, involving a new equation of state for solids. *J Metamorph Geol* 29:333–383
- Janák M, Froitzheim N, Yoshida K, Sasinková V, Nosko M, Kobayashi T, Hirajima T, Vrabec M (2015) Diamond in metasedimentary crustal rocks from Pohorje, Eastern Alps: a window to deep continental subduction. *J Metamorph Geol* 33:495–512
- Karabinos P (1984) Polymetamorphic garnet zoning from southeastern Vermont. *Am J Sci* 284:1008–1025
- Kienast JR, Lombardo B, Biino G, Pinarçon JL (1991) Petrology of very-high-pressure eclogitic rocks from the Brossasco-Isasca Complex, Dora-Maira Massif, Italian Western Alps. *J Metamorph Geol* 9:19–34
- Klug L, Froitzheim N (2021) Reuniting the Ötztal Nappe: the tectonic evolution of the Schneeberg Complex. *Int J Earth Sci*. <https://doi.org/10.1007/s00531-021-02127-4>
- Korsakov AV, Hutsebaut D, Theunissen K, Vandenabeele P, Stepanov AS (2007) Raman mapping of coesite inclusions in garnet from the Kokchetav Massif (Northern Kazakhstan). *Spectrochim Acta A* 68:1046–1052
- Kříž J, Degardin JM, Ferretti A, Hansch W, Gutiérrez Marco JC, Paris F, Piçarra D-Almeida JM, Robardet M, Schönlaub HP, Serpagli E (2003) Silurian stratigraphy and paleogeography of Gondwanan and Perunican Europe. *New York State Mus Bull* 493:105–178
- Kylander-Clark ARC, Hacker BR, Mattinson CG (2012) Size and exhumation rate of ultrahigh-pressure terranes linked to orogenic stage. *Earth Planet Sci Lett* 321–322:115–120
- Le Bayon B, Pitra P, Ballèvre M, Bohn M (2006) Reconstructing P-T paths during continental collision using multi-stage garnet (Gran Paradiso nappe, Western Alps). *J Metamorph Geol* 24:477–496

- Lenze A, Stöckhert B (2007) Microfabrics of UHP metamorphic granites in the Dora Maira Massif, western Alps—no evidence of deformation at great depth. *J Metamorph Geol* 25:461–475
- Luisier C, Baumgartner L, Schmalholz SM, Siron G, Vennemann T (2019) Metamorphic pressure variation in a coherent Alpine nappe challenges lithostatic pressure paradigm. *Nat Commun* 10:1–11
- Lü Z, Zhang L, Du J, Bucher K (2008) Coesite inclusions in garnet from eclogitic rocks in western Tianshan, northwest China: convincing proof of UHP metamorphism. *Am Mineral* 93:1845–1850
- Lü Z, Zhang L, Du J, Bucher K (2009) Petrology of coesite-bearing eclogite from Habutengsu Valley, western Tianshan, NW China and its tectonometamorphic implication. *J Metamorph Geol* 27:773–787
- Lü Z, Zhang LF, Chen ZY (2014) Jadeite- and dolomite-bearing coesite from western Tianshan, NW China. *Eur J Mineral* 26:245–256
- Manzotti P, Ballèvre M (2013) Multistage garnet in high-pressure metasediments: Alpine overgrowths on Variscan detrital grains. *Geology* 41:1151–1154
- Manzotti P, Pitra P, Langlade M, Ballèvre M (2015) Constraining *P-T* condition during thrusting of a higher pressure unit over a lower pressure one (Gran Paradiso, Western Alps). *J Metamorph Geol* 33:981–1002
- Manzotti P, Ballèvre M, Poujol M (2016) Detrital zircon geochronology in the Dora-Maira and Zone Houillère: a record of sediment travel paths in the Carboniferous. *Terra Nova* 28:279–288
- Manzotti P, Bosse V, Pitra P, Robyr M, Schiavi F, Ballèvre M (2018) Exhumation rates in the Gran Paradiso Massif (Western Alps) constrained by in situ U-Th-Pb dating of accessory phases (monazite, allanite and xenotime). *Contrib Mineral Petrol* 173:24
- Manzotti P, Ballèvre M, Pitra P, Schiavi F (2021) Missing lawsonite and aragonite found: *P-T* and fluid composition in meta-marls from the Combin Zone (Western Alps). *Contrib Mineral Petrol* 176:60. <https://doi.org/10.1007/s00410-021-01818-0>
- Manzotti P, Ballèvre M (2022) Chapter 8: Continental subduction in the Alps: from field data to kinematic models. In: Bellahsen N (ed) *Rosenberg C. Geodynamics of the Alps* Wiley, Hoboken
- Matsumoto N, Hirajima T (2000) Garnet in pelitic schist from a quartz-eclogite unit of the southern Dora-Maira massif, Western Alps. *Schweiz Mineral Petrogr Mitt* 80:53–62
- Mattirolo E, Novarese V, Franchi S, Stella A (1913) *Carta Geologica d'Italia alla scala 1:100.000, Foglio 55 Susa*, Geol Surv It
- Mattirolo E, Novarese V, Franchi S, Stella A (1951) *Carta Geologica d'Italia alla scala 1:100.000, Foglio 67 Pinerolo*. Geol Surv It
- Mazzucchelli ML, Angel RJ, Alvaro M (2021) EntraPT: an online platform for elastic geothermobarometry. *Am Mineral* 106:830–837
- Michard A, Henry C, Chopin C (1995) Structures in UHPM: a case study from the Alps. In: Coleman RG, Wang X (eds) *Ultrahigh pressure metamorphism*. Cambridge University Press, Cambridge, pp 132–158
- Michard A, Schmid SM, Lahfid A, Ballèvre M, Manzotti P, Chopin C, Iaccarino S, Dana D (2022) The Maira-Sampeyre and Val Grana Allochthons (south Western Alps): review and new data on the tectonometamorphic evolution of the Briançonnais distal margin. *Swiss J Geosci* 115:19 (in press)
- Nosenzo F, Manzotti P, Poujol M, Ballèvre M, Langlade M (2022) A window into an older orogenic cycle: *P-T* conditions and timing of the pre-Alpine history of the Dora-Maira Massif (Western Alps). *J Metamorph Geol* 40:789–821. <https://doi.org/10.1111/jmg.12646>
- Orozbaev R, Hirajima T, Bakirov A, Takasu A, Maki K, Yoshida K, Sakiev K, Bakirov A, Hirata T, Tagiri M, Togonbaeva A (2015) Trace element characteristics of clinozoisite pseudomorphs after lawsonite in talc-garnet-chloritoid schists from the Makbal UHP Complex, northern Kyrgyz Tian-Shan. *Lithos* 226:98–115
- Piana F, Fioraso G, Irace A, Mosca P, d'Atri A, Barale L, Falletti P, Monegato G, Morelli M, Tallone S, Vigna GB (2017) Geology of Piemonte region (NW Italy, Alps-Apennines interference zone). *J Maps* 13:395–405
- Pitra P, Ballèvre M, Ruffet G (2010) Inverted metamorphic field gradient towards a Variscan suture zone (Champocéaux Complex, Armorican Massif, France). *J Metamorph Geol* 28:183–208
- Pognante U, Sandrone R (1989) Eclogites in the northern Dora-Maira Nappe (Western Alps, Italy). *Min Pet* 40:57–71
- Reinecke T (1991) Very-high-pressure metamorphism and uplift of coesite-bearing metasediments from the Zermatt-Saas zone, Western Alps. *Eur J Mineral* 3:7–17
- Reinecke T (1998) Prograde high- to ultrahigh-pressure metamorphism and exhumation of oceanic sediments at Lago di Cignana, Zermatt-Saas Zone, western Alps. *Lithos* 42:147–189
- Rolfo F, Compagnoni R, Wu X, Xu S (2004) A coherent lithostratigraphic unit in the coesite-eclogite complex of Dabie Shan, China: geologic and petrologic evidence. *Lithos* 73:71–94
- Rubatto D, Hermann J (2001) Exhumation as fast as subduction? *Geology* 29:3–6
- Sandmann S, Nagel TJ, Herwartz D, Fonseca ROC, Kurzwaski RM, Munker C, Froitzheim N (2014) Lu-Hf garnet systematics of a polymetamorphic basement unit: new evidence for coherent exhumation of the Adula Nappe (Central Alps) from eclogite-facies conditions. *Contrib Mineral Petrol* 168:1075
- Sandrone R, Borghi A (1992) Zoned garnets in the northern Dora-Maira Massif and their contribution to a reconstruction of the regional metamorphic evolution. *Eur J Mineral* 4:465–474
- Sandrone R, Cadoppi P, Sacchi R, Vialon P (1993) The Dora-Maira massif. In: Von Raumer JF (ed) *Pre-Mesozoic geology in the Alps*. Springer, Berlin, pp 317–325
- Schmid SM, Fügenschuh B, Kissling E, Schuster R (2004) Tectonic map and overall architecture of the Alpine orogeny. *Eclogae Geol Helv* 97:93–117
- Smye AJ, Greenwood LV, Holland TJB (2010) Garnet-chloritoid-kyanite assemblages: eclogite facies indicators of subduction constraints in orogenic belts. *J Metamorph Geol* 28:753–768
- Smith DC (1984) Coesite in clinopyroxene in the Caledonides and its implications for geodynamics. *Nature* 310:641–644
- Tagiri M, Bakirov A (1990) Quartz pseudomorph after coesite in garnet from a garnet-chloritoid-talc schist, Northern Tien-Shan, Kirghiz SSR. *Proc Jpn Assoc Sci* 66:135–139
- Taguchi T, Kouketsu Y, Igami Y, Kobayashi T, Miyake A (2021) Hidden intact coesite in deeply subducted rocks. *Earth Planet Sci Lett* 558:116763
- Thompson AB, Connolly JAD (1990) Metamorphic fluids and anomalous porosities in the lower crust. *Tectonophysics* 182:47–55
- Vaughan-Hammon JD, Luisier C, Baumgartner LP, Schmalholz SM (2021) Peak Alpine metamorphic conditions from staurolite-bearing metapelites in the Monte Rosa nappe (Central European Alps) and geodynamic implications. *J Metamorph Geol* 39:897–917
- Vialon P (1966) *Étude géologique du massif cristallin Dora-Maira, Alpes Cottiennes Internes, Italie*. Travaux du Laboratoire de Géologie de la Faculté des Sciences de Grenoble, Mémoires, 4. <https://hal.archives-ouvertes.fr/tel-00723197>
- Vrabec M, Janák M, Froitzheim N, Hoog JCM (2012) Phase relations during peak metamorphism and decompression of the UHP kyanite eclogites, Pohorje Mountains (Eastern Alps, Slovenia). *Lithos* 144–145:40–55
- Wain A (1997) New evidence for coesite in eclogite and gneisses: defining an ultrahigh-pressure province in the Western Gneiss region of Norway. *Geology* 25:927–930
- Yardley BWD, Condliffe E, Lloyd GE, Harris HM (1996) Polyphase garnets from western Ireland: two-phase intergrowths in the grossular-almandine series. *Eur J Mineral* 8:383–392

Zhang L, Ellis DJ, Arculus RJ, Jiang W, Wei C (2003) 'Forbidden zone' subduction of sediments to 150 km depth—the reaction of dolomite + magnesite in the UHPM metapelites from western Tianshan, China. *J Metamorph Geol* 21:523–529

**Publisher's Note** Springer Nature remains neutral with regard to jurisdictional claims in published maps and institutional affiliations.